AKADÉMIAI KIADÓ

Central European Geology

DOI:
10.1556/24.2022.00113

RESEARCH ARTICLE

Petrographic evidences of open-system magmatic processes in the felsic rocks of the northern part of the Ditrău Alkaline Massif (Eastern Carpathians, Romania)

LUCA KIRI[1]*, MÁTÉ SZEMERÉDI[1,2] and ELEMÉR PÁL-MOLNÁR[1,2]

[1] 'Vulcano' Petrology and Geochemistry Research Group, Department of Mineralogy, Geochemistry and Petrology, University of Szeged, Szeged, Hungary

[2] MTA-ELTE Volcanology Research Group, Budapest, Hungary

Received: July 23, 2021 • Accepted: February 20, 2022

ABSTRACT

Over the almost 190 years-long research of the Ditrău Alkaline Massif (Eastern Carpathians, Romania), felsic rocks have been regarded as homogeneous, uniform units of the igneous complex. Nevertheless, our detailed textural study revealed that the felsic suite (diorite–alkaline feldspar syenite and nepheline-bearing syenite–granite series) cropping out north of the Jolotca Creek valley is more heterogenous at micro-scale than previously thought. This heterogeneity partly derives from abundant mafic mineral-rich clusters; nevertheless, felsic minerals also exhibit various, remarkable textural features. Outcrop to micro-scale traits of felsic crystal settling, mafic mineral aggregates and flow fabrics along with metamorphic country rock xenoliths suggest that the studied rocks crystallized under dynamic magmatic conditions. Cumulate formation, shear flow, convection currents as well as various open-system magmatic processes (e.g., magma recharge, magma mixing and mingling, crystal or mush transfer and recycling, country rock assimilation) played a significant role in the petrogenesis of the examined felsic suite.

Based on field observations as well as on the microtextural relationship of the minerals, two major groups of felsic rocks were distinguished: (1) felsic rocks (lacking or containing sparse mafic minerals) spatially associated with mafic rocks and (2) felsic rocks (with mafic minerals and clots) spatially unassociated with mafic rocks. Rocks of the former group are dominated by plagioclase, accompanied by minor alkaline feldspar, biotite and accessory titanite. Distinct structural and textural features suggest the physical accumulation of the rock-forming phases. Such textural properties can also be observed in some rocks of the second group. Isolated mafic minerals are rather scarce in the latter; nevertheless, different types of aggregates made up of either identical or various mafic phases are more common. Clustered minerals are either intact or show different stages of alteration.

A detailed petrographic study of the above-mentioned peculiarities has been implemented in order to define their potential origin(s) and petrogenetic significance.

KEYWORDS

Ditrău Alkaline Massif, entrainment, felsic clots, felsic cumulates, hybridization, mafic clots, pseudomorphism, replacement

*Corresponding author. 'Vulcano' Petrology and Geochemistry Research Group, Department of Mineralogy, Geochemistry and Petrology, University of Szeged, 2 Egyetem Str., H-6722, Szeged, Hungary.
E-mail: kiri.luca@gmail.com

INTRODUCTION

The Ditrău Alkaline Massif (DAM) is a unique locality with a presently tilted vertical cross-section of a preceding alkaline magma storage system (Pál-Molnár et al., 2015a) exposing different rock types on a spectrum of ultramafic cumulates to granitoid rocks. The outcrops provide excellent *in-situ* insight into the different stages of the evolution of the alkaline igneous suite.

Felsic rocks have been regarded – both at macro and micro-scale – as homogeneous, uniform units of the DAM throughout almost the entire research history of the massif. Recently, some studies (e.g., Batki et al., 2018; Heincz et al., 2018; Ódri et al., 2020) drew attention to distinct structural, textural and geochemical features, implying open-system processes that had operated during the formation of the examined felsic rocks. Application of *in-situ* geochemical analysis made a significant contribution to the appropriate interpretation of these rocks. However, in spite of the new findings of the above-cited articles, several questions regarding the genesis of the felsic suite (e.g., provenance, composition and evolution of the parental magma) have still remained unanswered.

Pál-Molnár et al. (2015a) revealed that accumulation of mafic minerals has played a crucial role in the petrogenesis of some rock types of the DAM (e.g., olivine-rich cumulate, amphibole- and pyroxene-rich cumulate, amphibole-rich cumulate). The existence of a hypothetic felsic cumulate pile in the massif has been proposed by Heincz et al. (2018). Furthermore, Ódri et al. (2020) presumed that some felsic rocks (e.g., syenite and quartz syenite) could have been formed by crystal accumulation as well.

According to Chappell et al. (1987), the viscosity of felsic melts does not favor the segregation of crystals. However, 1–3% volatile-content may decrease the viscosity of felsic magmas so effectively that it allows crystals to settle and accumulate on the floor of a magma chamber (e.g., Dingwell et al., 1985, 1996; Baker, 1996, 1998). Furthermore, crystals could also separate from high-temperature felsic melts with low volatile-content, since melt viscosity decreases with increasing temperature (Clemens et al., 1997; Dingwell et al., 1996). Wiebe et al. (2002), Miller and Miller (2002) as well as Collins et al. (2006) recognized that in the case of felsic systems, settling of multi-crystalline aggregates is more effective than sinking of single crystals. Numerous structural and textural attributes may point to the mechanical accumulation of the felsic rock-forming minerals (Vernon and Paterson, 2006; Vernon and Collins, 2011).

Rocks of the diorite–alkaline feldspar syenite and nepheline-bearing syenite–granite series not only comprise isolated ferromagnesian phases but also include mafic clots (also known as: aggregates, blobs, clumps, clusters, lumps, nodules) containing multiple crystals of either identical or various ferromagnesian minerals.

Several theories and interpretations can be found in the literature concerning the origin of mafic aggregates: (1) mineral accumulation, (2) magma mixing and mingling and (3) the involvement of exotic (e.g., crustal or restitic) materials.

Cumulate or chilled-margin phases originating from the border zones of the pluton, incorporated as solid or partly solid enclaves (Wiebe et al., 1997) are also known as cognate (autolith) inclusions (Kumar and Singh, 2014). Such enclaves are cogenetic with the host rock and consist of early-formed – mostly mafic – mineral phases identical to those of the enclosing rock (Hughes, 1982; Wall et al., 1987). Convection currents are highly capable of dragging and transporting crystal clots and fragments. These aggregates could survive the high temperature in the interior of the chamber without being dissolved; thus, they could be preserved as (recrystallized) autolithic enclaves (Bea, 2010). Klaver et al. (2017) defined the term "microcumulate" as a cluster of 5–50 crystals that are only recognizable in thin section. They often exhibit non-equilibrium textures, such as reaction-replacement of ferromagnesian minerals along cleavage planes, rims and fractures.

Mafic microgranular enclaves (MME) can be formed by (1) the replenishment of the magma chamber (Frost and Mahood, 1987; Wiebe and Collins, 1998; Vernon and Paterson, 2006; Vernon and Collins, 2011); (2) break-up of a basal sheet in a compositionally layered intrusion (Wiebe et al., 1997); (3) magma mixing and mingling (Kumar and Singh, 2014). Disruption of the enclaves may lead to the formation of mafic clots (Wiebe, 1973). Nevertheless, single crystals or mineral aggregates of more basic composition can also be incorporated into the enclave-bearing felsic magma (Didier, 1987). Micro-enclaves (up to 1 cm) are subspherical clusters of ferromagnesian minerals, along with titanite and Ca-plagioclase. Convection currents may drag and carry these phases and distribute them throughout the magma storage system. The presence of micro-enclaves and contrasting zoning of neighboring feldspars implies the initial, practically thorough mixing phase (Fernandez and Barbarin, 1991). Interaction between mafic magma-derived crystals (e.g., pyroxene) and a volatile-rich, felsic magma leads to the formation of polycrystalline amphibole-rich clusters (Vernon, 1984, 1990; Castro and Stephens, 1992; Zorpi et al., 1991). Further hybridization (hydration and mass-transfer of the chemical components) may result in the replacement of amphibole by biotite (Tate et al., 1997; Ubide et al., 2014).

The residual source material (restite) is a patch of unmelted mafic substance (single crystals or small mineral aggregates) from the source region that got carried by the ascending magma (White and Chappell, 1977). During this process, the crystals either remain intact (primary restite) (Chappell et al., 1987) or recrystallize due to the lower P-T and more hydrous conditions (Wall et al., 1987) in order to reach equilibrium with the host magma (secondary restite). Restitic minerals can be derived either straight from the source region following partial melting or from the host magma-induced dismemberment of the restite enclaves (Huang et al., 2018). According to Chappell et al. (1987), Presnall and Bateman (1973), White and Chappell (1977) as well as Chappell (1978), many of the amphibole and biotite crystals occurring as clots in granites are products of reaction between restitic pyroxenes and the host granitic melt.

The detailed petrographic study presented herein is the first step in the revision and reinterpretation of the felsic rocks (diorite–alkaline feldspar syenite and nepheline-bearing syenite–granite suite) occurring in the northern part of the DAM (the region north of the Jolotca Creek, bordered by the Teasc and the Rezu Mare Creeks), based on a systematically collected and documented new set of samples. The aim of this paper is to shed light on and emphasize

the importance of micro-scale textural features that bear important information on the genesis of the studied rocks. The examined felsic rocks seem to be of more considerable petrographic complexity than presented in previous interpretations. The objective here is to illustrate and describe the diverse petrographic characteristics of the studied felsic rocks and to introduce a preliminary discussion concerning their genetic peculiarities.

GEOLOGIC SETTING

The Ditrău Alkaline Massif covers an area of approximately 225 km^2 in the Eastern Carpathians, Dacia Mega-Unit (Romania; Fig. 1A) and makes up the southern and southwestern parts of the Giurgeu Mountains. The DAM comprises various rock types occurring in an intricate structural

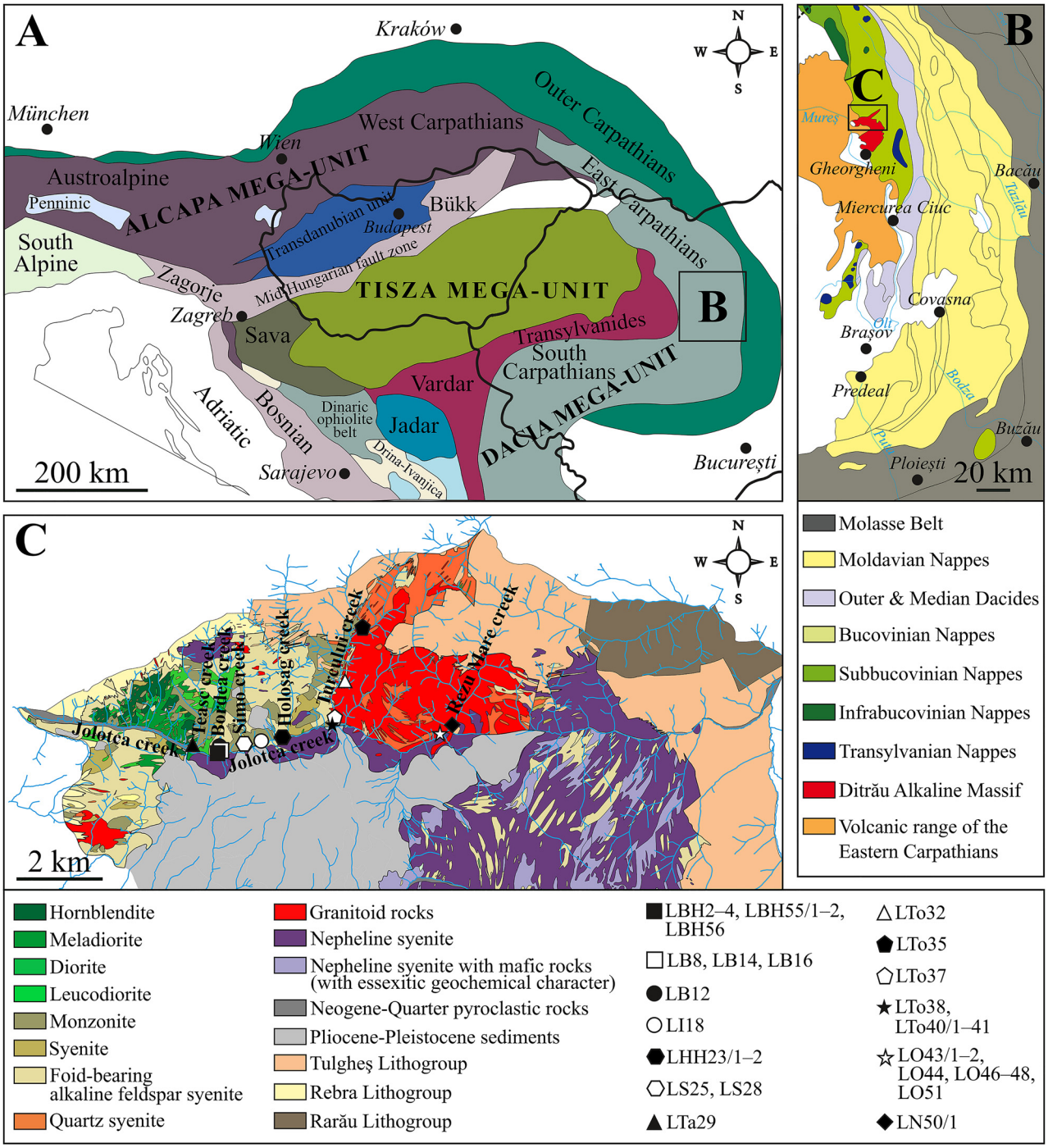

Fig. 1. (A) Location of the Ditrău Alkaline Massif (DAM) in the structural framework of the Alpine–Carpathian–Dinaric region (after Pál-Molnár, 2010). (B) Position of the DAM in the Alpine structural units of the Eastern Carpathians (Săndulescu et al., 1981, modified). (C) Schematic geologic map of the northern part of the DAM, exhibiting sampling sites (Pál-Molnár et al., 2015a)

framework: ultramafic cumulates (olivine-rich cumulate, amphibole- and pyroxene-rich cumulate, amphibole-rich cumulate), alkali gabbro, alkali diorite, monzodiorite, monzonite, monzosyenite, syenite, nepheline syenite, quartz syenite and alkali granite (Fig. 1C). The above-mentioned rock bodies are intersected by lamprophyre, syenite and tinguaite dykes (Pál-Molnár, 2000; Batki et al., 2014; Pál-Molnár et al., 2015a, b).

The igneous event took place during the Middle–Late-Triassic (Pál-Molnár et al., 2021) at the southwestern margin of the East European craton and can be attributed to an extensional, rift-related, intra-plate tectonic environment. The DAM had intruded into the Variscan metamorphic rocks of the Eastern Carpathians that were exposed to subsequent nappe-forming Alpine tectonic phases (Fig. 1B). The Cretaceous (Austrian) tectogenesis resulted in an east-verging nappe system. In the literature it is cited as Median Dacides (Săndulescu, 1984) or as Eastern Getides (Balintoni, 1997). The Median Dacides are composed of three Alpine nappes (Infrabucovinian, Subbucovinian and Bucovinian Nappes), comprising pre-Alpine metamorphic rocks and Permo-Mesozoic cover sequences (Săndulescu, 1984). The Subbucovinian and Bucovinian Nappes are made up of pre-Alpine, petrographically identical tectonic units (Rodna, Pietrosu Bistriței, Putna and Rarău Nappes) of western vergence (Balintoni et al., 1983; Vodă and Balintoni, 1994; Balintoni, 1997).

Within a structural aspect the DAM forms part of the Bucovinian Nappe (Fig. 1B) and is directly related to four of its pre-Alpine metamorphic terranes (Bretila, Tulgheș, Negrișoara and Rebra Lithogroups; Balintoni et al., 2014).

The massif and the Subbucovinian Nappe are divided by a tectonic unconformity, since the DAM was uprooted amidst the Alpine tectonic processes and was slit by the Bucovinian shear zone at a depth of approximately 1800–2000 m (Kräutner and Bindea, 1995).

SAMPLING AND ANALYTICAL TECHNIQUES

To better understand the felsic rocks and their relationship with other rock types of the Ditrău Alkaline Massif, a set of new, systematically collected and documented samples has been acquired. The fieldwork took place in late 2019 and covered the northern part of the DAM (the area north of the Jolotca Creek, bounded by the Teasc and the Rezu Mare Creeks). Exposures are rather poor (Fig. 2A) due to dense vegetation and recent recultivation; thus, sampling points were mostly situated in valleys of creeks and on hillsides (Figs 1C and 2). Samples were collected from *in-situ* outcrops. All characteristic felsic rock types as well as metamorphic country rocks of the northern area were sampled and the most representative specimens were studied. Samples were named after their sampling locality (i.e., name of creeks). Out of the 49 specimens, 46 thin sections were prepared at the Department of Petrology and Geochemistry, Eötvös Loránd University, Budapest, Hungary. Petrographic observations were implemented on both hand specimens and on thin sections at the Department of Mineralogy, Geochemistry and Petrology, University of Szeged, Szeged, Hungary. Thin sections were investigated under Olympus BX41 and Brunel SP300P optical microscopes. Mineral phases were determined using a THERMO Scientific DXR Raman microscope. Modal compositions (V/V%) in petrographic descriptions were estimated using the JMicroVision image processing software (Roduit, 2019) by counting 2000 randomly positioned points in each thin section. Backscattered electron (BSE) images were taken with an AMRAY 1830 SEM equipped with an EDAX PV 9800 EDS detector at the Department of Petrology and Geochemistry, Eötvös Loránd University, Budapest, Hungary. BSE imaging was applied to reveal compositional zoning as well as microtextural and reaction relations among the adjacent mineral phases.

RESULTS

Field observations

The contact between the mafic and felsic rocks cannot be directly traced in the study area due to the adverse exposures and soil formation processes (Fig. 2A); therefore, their field relationship is not unambiguous.

The macroscopic and microscopic appearances of the studied rocks are remarkably complex. Felsic rocks display various petrographic features (e.g., grain size, type of mafic minerals and/or clots, degree of alteration and/or replacement of ferromagnesian components, textural orientation) in different parts of the massif. Decimeter–meter-scale mafic microgranular enclaves have not been observed; nevertheless, smaller-sized mafic aggregates (Fig. 3A–D) and metamorphic country rock xenoliths are common (Figs 2D and 3E, F). Several late-stage mafic (lamprophyre) and felsic (alkaline feldspar syenite, syenite, monzonite and quartz syenite) dykes crosscut the felsic igneous bodies (Fig. 2E).

Petrography

Detailed petrographic description and interpretation of the mafic rocks of the study area are the subject of companion studies (e.g., Pál-Molnár, 2000; Pál-Molnár et al., 2015a). Hence, the attributes of felsic rocks are emphasized and discussed in detail and only the relevant field, mineralogical and textural observations of the mafic rocks, are interpreted in this paper.

Many significant textural characteristics of the studied rocks can only be revealed by classic polarized-light microscopic investigations; thus, the presented descriptions are based on optical microscopic observations. However, features that are controlled by the chemical composition may only be unraveled by SEM imaging. Hence, the optical microscopic analyses were complemented by the interpretation of SEM images.

The felsic rocks can be classified into two major groups in line with their spatial occurrence and petrographic features (Fig. 4).

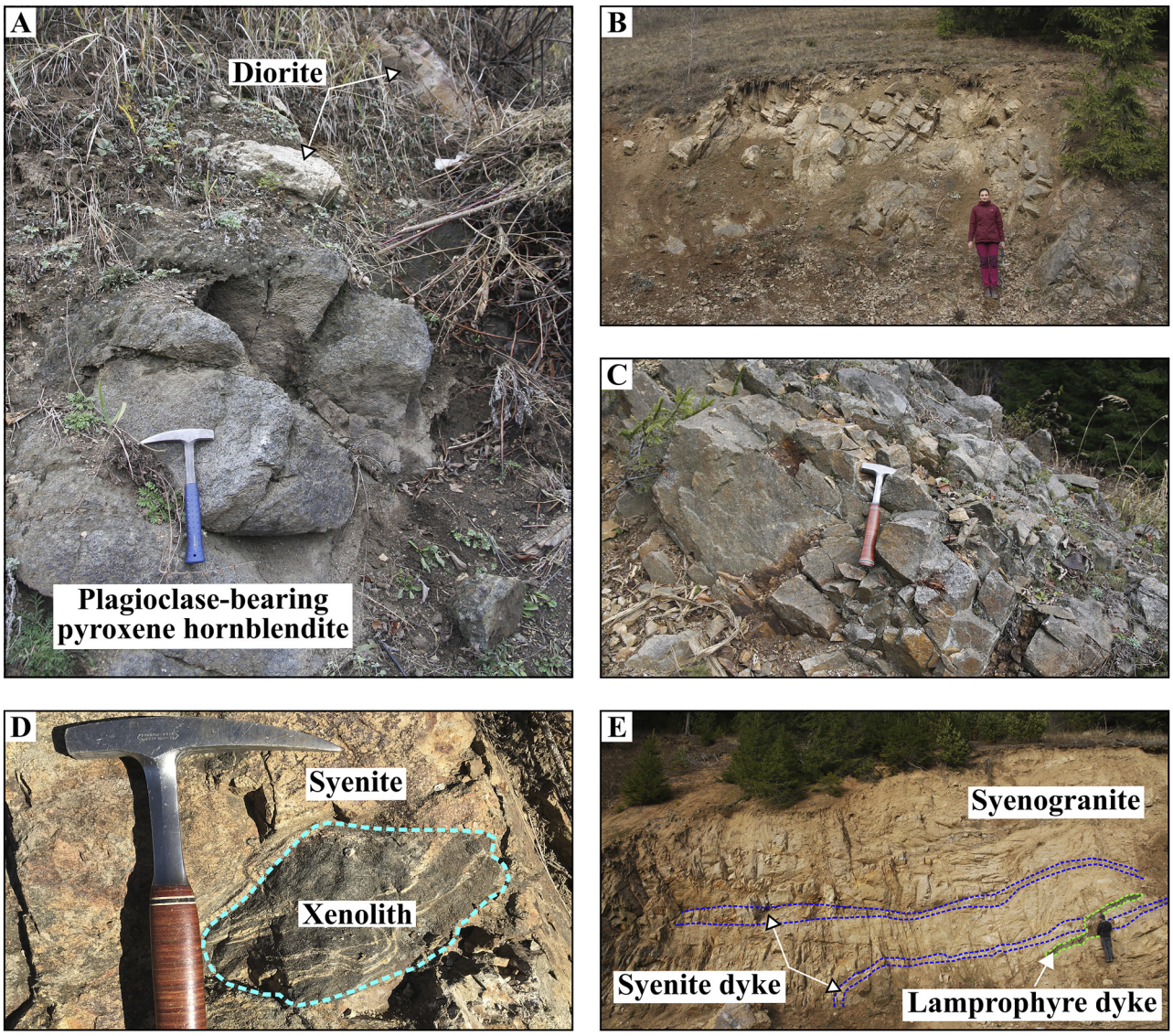

Fig. 2. Outcrops of the studied felsic rocks. (A) Plagioclase-bearing pyroxene hornblendite overlain by diorite. (B) and (C) Monzonite and monzogranite exposures, respectively. (D) Metamorphic country rock xenolith (marked by turquoise dashed line) enclosed by syenite. (E) Syenogranite intruded by syenite and lamprophyre dykes. The former is highlighted by blue, whereas the latter is distinguished by green dashed lines

Group 1 – Felsic rocks (lacking or containing sparse mafic minerals) spatially associated with mafic rocks (hillside west of the Bordea Creek)

The associated mafic rock is composed of plagioclase, green amphibole, biotite, scarce clinopyroxene and accessory phases (apatite, titanite) and shows evident textural features of mineral accumulation processes (Fig. 6A). Based on its fabric and paragenesis, the rock can be classified as plagioclase-bearing pyroxene hornblendite.

Felsic rocks of this group (Fig. 4) are white, medium to coarse-grained, phaneritic, inequigranular and composed mainly of plagioclase, minor amount of alkaline feldspar, accompanied by biotite flakes in variable amount (up to 9 V/V%) (Table 1). Titanite is the most common accessory mineral. In accordance with their modal composition, the studied felsic rocks can be regarded as diorite (Fig. 5).

Idiomorphic–hypidiomorphic plagioclase (400–2,500 μm) is the dominant phase, making up almost 90 V/V% of the studied rocks (Fig. 6A, B). Idiomorphic–hypidiomorphic apatite (90–500 μm) and titanite (80–400 μm) occur as inclusions within. The typical zoning pattern of plagioclase is defined by a variously altered (sericitized), occasionally resorbed, sieve-textured core mantled by a fresh, inclusion-free, unaltered rim (Fig. 6C, D). Larger-sized (up to 9 mm), idiomorphic–hypidiomorphic plagioclase megacrysts are also common (Fig. 6B). Idiomorphic–xenomorphic alkaline feldspar (300–800 μm) often shows perthitic texture and occurs in minor amount (2–8 V/V%). It fills up the intergranular space between the framework of larger-sized plagioclase

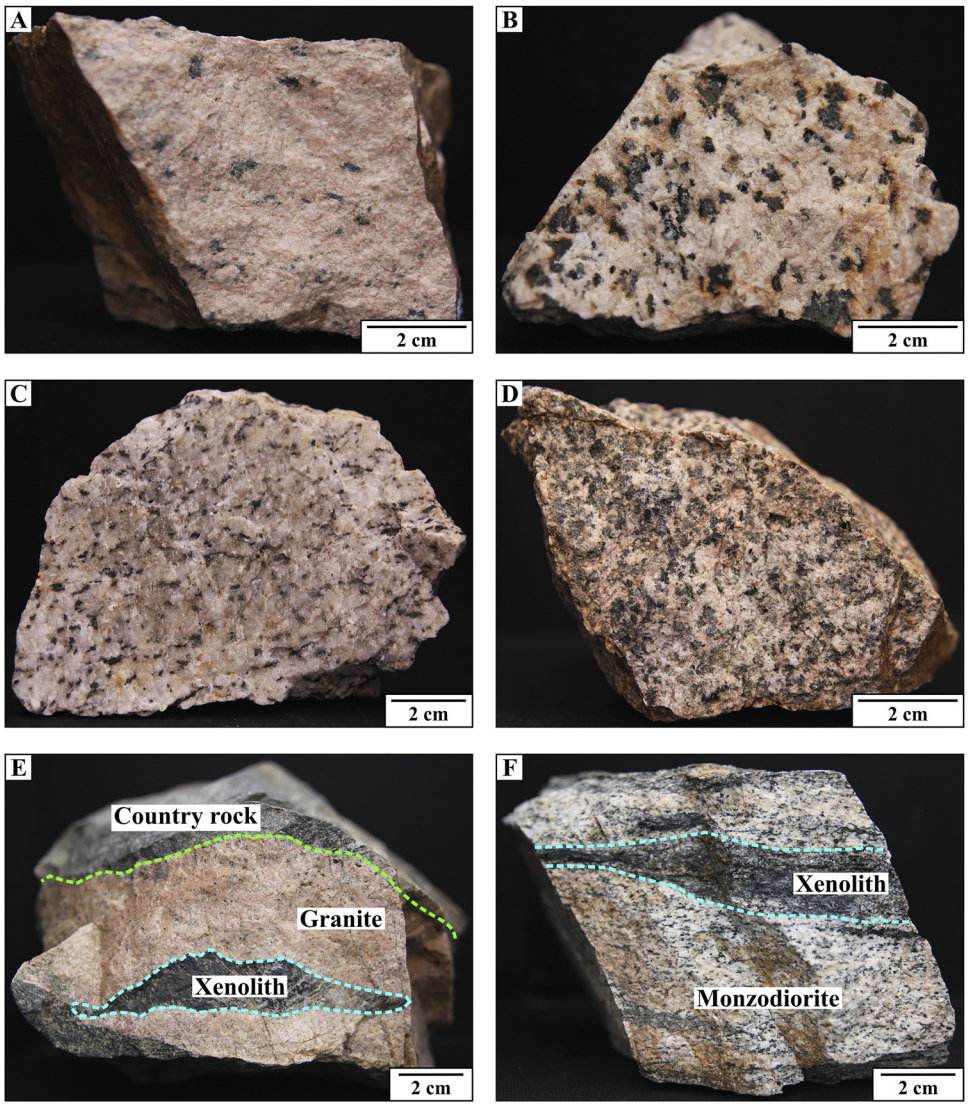

Fig. 3. Characteristic macroscopic textural features of some of the studied felsic rocks. Mafic clots in (A) monzonite dyke, (B) monzonite, (C) nepheline-bearing syenite and (D) monzonite. (E) Hornfels xenolith enclosed by granite along the contact with the metamorphic country rock. (F) Hornfels xenolith in monzodiorite with oriented texture. Margins of the xenoliths are highlighted by turquoise, whereas the contact with the metamorphic wall rock is marked with green dashed lines

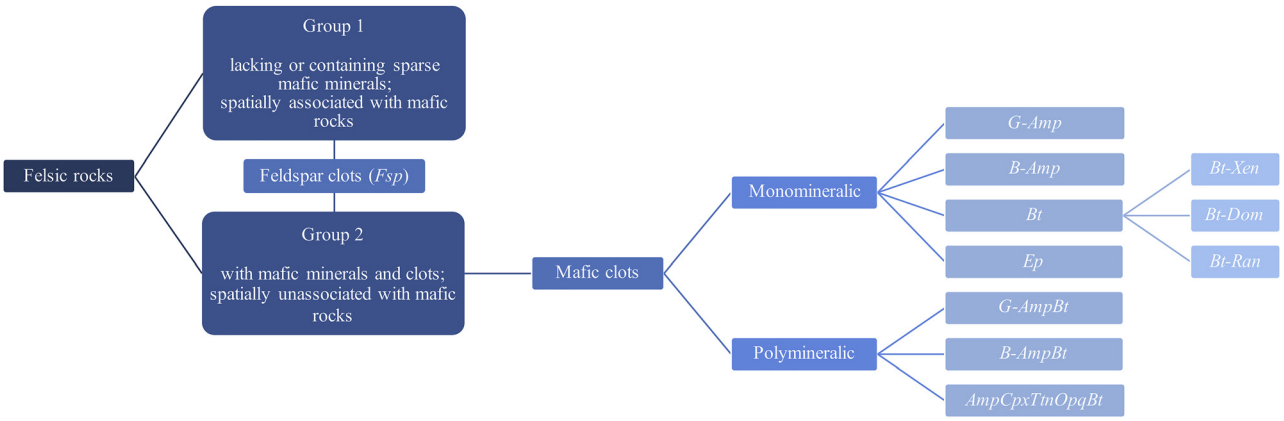

Fig. 4. Tree diagram illustrating the hierarchy of the studied rocks and of the various types of mafic aggregates

Table 1. Sampling locality and the modal composition (V/V%, without mafic clots) of the investigated felsic rocks of the Ditrău Alkaline Massif

Group	Sample	Rock type	Locality and GPS coordinates	Modal composition of the felsic host without mafic clots (V/V%)												
				Pl	Afs	Qtz	Neph	Cpx	G-Amp	B-Amp	Act	Bt	Ms	Ttn	Opq	Ep
1	LB8	Diorite	Bordea creek 46.86246, 25.51698	87	2							9		1		1
	LB16	Diorite with oriented texture	Bordea creek 46.86235, 25.51704	85	8							4	2			1
2	LBH2	Monzodiorite with oriented texture	Hillside west of the Bordea creek 46.86200, 25.51558	62	31				3			2		1	<1	
	LBH3	Monzonite	Hillside west of the Bordea creek 46.86202, 25.51570	51	43							4		<1	<1	1
	LBH4	Monzonite dyke	Hillside west of the Bordea creek 46.86198, 25.51574	42	56							<1		<1	<1	<1
	LB12	Monzonite	Bordea creek 46.86376, 25.51694	47	51							2				
	LB14	Monzonite dyke with oriented texture	Bordea creek 46.86257, 25.51718	46	50							1		1		2
	LI18 fine-grained	Monzonite with oriented texture	Behind the school in Jolotca 46.86448, 25.52762	43	53				1			2		1		
	LI18 coarse-grained	Monzonite	Behind the school in Jolotca 46.86448, 25.52762	50	43				6			<1		<1		
	LHH23/1	Monzonite	Hillside west of the Holoșag creek 46.86579, 25.53452	56	38							6				
	LHH23/2	Monzonite	Hillside west of the Holoșag creek 46.86579, 25.53452	42	55							2		<1	<1	
	LS25	Syenite with oriented texture	Simo creek 46.86425, 25.52344	31	64				<1			4		<1		
	LS28	Nepheline-bearing syenite with oriented texture	Simo creek 46.86456, 25.52324	25	70		2		1			1		1		
	LTa29	Monzonite	Teasc creek 46.86344, 25.50844	42	51				2		1	1		2	1	
	LTo32	Monzogranite	Turcului creek 46.87757, 25.55223	43	31	20			2			4				
	LTo35	Monzogranite	Turcului creek 46.8887, 25.55766	36	35	24			3			2				
	LTo37	Monzogranite	Turcului creek 46.86908, 25.54919	32	41	22			<1		4	<1		<1	<1	
	LTo38	Quartz syenite	Turcului creek 46.86829, 25.54906	11	72	15						2				
	LTo40/1	Monzonite	Turcului creek 46.86803, 25.54850	34	62	2						<1		<1	1	
	LTo41	Syenite	Turcului creek 46.86815, 25.54878	24	76											

(continued)

Table 1. Continued

Group	Sample	Rock type	Locality and GPS coordinates	Modal composition of the felsic host without mafic clots (V/V%)												
				Pl	Afs	Qtz	Neph	Cpx	G-Amp	B-Amp	Act	Bt	Ms	Ttn	Opq	Ep
	LO43/1	Quartz syenite	Jolotca creek 46.86636, 25.58108	20	72	6				1		<1				
	LO43/2	Quartz monzonite	Jolotca creek 46.86636, 25.58108	35	45	16			<1	<1		3				
	LO44	Quartz syenite dyke	Jolotca creek 46.86637, 25.58113	24	56	17		<1		<1		2				
	LO46	Syenite dyke	Jolotca creek 46.86652, 25.58135	40	50			<1		<1		9	<1			
	LO47	Syenite dyke	Jolotca creek 46.86653, 25.58107	22	64							6	8			
	LO48	Syenogranite	Jolotca creek 46.86658, 25.58144	22	56	21				<1		<1			<1	
	LN50/1	Granite + hornfels country rock	Rezu Mare creek 46.86842, 25.58544	20	28	46						6				
	LO51	Alkaline feldspar syenite dyke with oriented texture	Jolotca creek 46.86651, 25.58117	8	78							3	11			
	LBH55/1	Monzodiorite with oriented texture + hornfels xenolith	Hillside west of the Bordea creek 46.86196, 25.51556	71	22							7				
	LBH55/2	Monzodiorite with oriented texture	Hillside west of the Bordea creek 46.86196, 25.51556	61	30							8	<1			<1
	LBH56	Monzonite	Hillside west of the Bordea creek 46.86196, 25.51564	35	63							2				

Abbreviations: Pl – plagioclase, Afs – alkaline feldspar, Qtz – quartz, Neph – nepheline, Cpx – clinopyroxene, G-Amp – green amphibole, B-Amp – blue amphibole, Act – actinolite (secondary), Bt – biotite, Ms – muscovite (secondary), Ttn – titanite, Opq – opaque minerals, Ep – epidote (secondary)

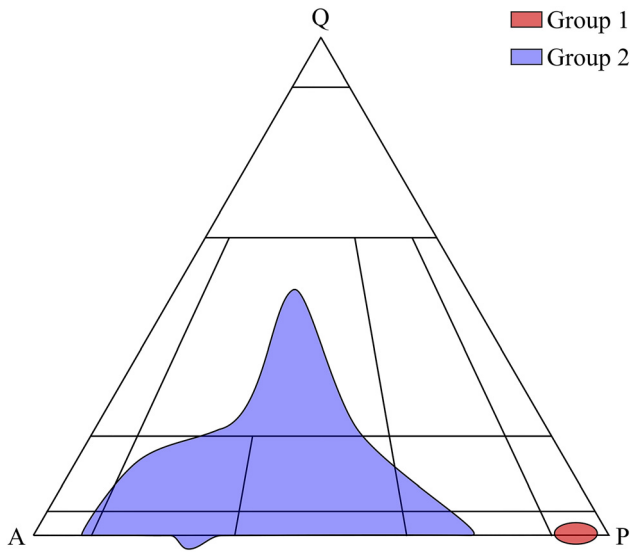

Fig. 5. QAP diagram illustrating the classification of the studied felsic rocks based on their modal composition (Le Maitre et al., 2002). Abbreviations: Q – quartz, A – alkaline feldspar, P – plagioclase

crystals; however, it sporadically appears as a rock-forming phase along with plagioclase (Fig. 6A–C). Feldspars in contact generally have straight crystal faces and are frequently aligned parallel to them; thus, forming aggregates of multiple crystals and defining an oriented texture as well (Fig. 6A, C). Furthermore, impingement of feldspar grains with separate cores is also prevalent (Fig. 6D, marked by the red arrow). There are clusters of multiple, molded, sericitized, sieve-textured feldspar crystals that are mantled by a common, inclusion-free overgrowth (Fig. 6D, marked by the yellow arrow).

Biotite (200–5,000 µm) is hypidiomorphic–xenomorphic (Fig. 6A, B, D); sagenitic texture as well as idiomorphic–hypidiomorphic apatite (80–300 µm) and titanite inclusions are its common features (Fig. 6D). Titanite is completely or partially enclosed by biotite and has two generations (90–300 and 600–1,000 µm sized). Biotite occurs sporadically (Fig. 6B): some domains are completely devoid of it, whereas in other areas it is concentrated into local accumulations of multiple grains (showing no evidence of a touching framework).

Idiomorphic–hypidiomorphic apatite (~200 µm) and titanite appear along the main rock-forming phases as well (~1 V/V%) (Fig. 6B). Interstitial titanite has two populations: 200–600 and 900–1,500 µm in size. Secondary minerals are represented by muscovite (0–2 V/V%) and epidote (1 V/V%). Fine-grained epidote either forms intergrowths with sagenitic biotite or occurs as inclusion. It also fills up the space between feldspars in the form of well-developed crystals or as microcrystalline aggregates (2 V/V%) (Fig. 6A, C). Epidote, along with titanite is present as vein-filling as well.

The contact between the mafic and felsic rocks in the same outcrop can only be traced in a single hand specimen. Nevertheless, this sample perfectly preserves the continuous transition between the two rock types, forming an interlocking texture. Signs of sharp, abrupt changes or intrusive processes have not been identified (Fig. 6A).

Group 2 – Felsic rocks (with mafic minerals and clots) spatially unassociated with mafic rocks (area between the Teasc and the Rezu Mare Creeks)

Felsic rocks of this group (Fig. 4) are white to (pale) pink and have medium to coarse-grained, phaneritic, (in)equigranular texture (some of them contain megacrysts of up to 11 mm) (Fig. 3A–D). They cover the entire spectrum of felsic rocks from alkaline feldspar syenite to monzodiorite as well as from nepheline-bearing syenite to granite (Fig. 5). These rocks vary in the modal proportion of felsic minerals and the presence or absence of feldspathoids and quartz (Table 1). Alkaline feldspar (orthoclase and microcline) commonly exhibits perthitic microtexture. Most of the plagioclases have a distinct, somewhat resorbed, sericitized, sieve-textured core rimmed by an inclusion-free mantle. Nevertheless, some rocks contain a minor amount of reverse-zoned feldspar crystals. It is common that smaller plagioclase crystals are enclosed by alkaline feldspar. Plagioclases in contact with alkaline feldspar exhibit irregular grain boundaries. Additional accessory phases (most commonly apatite, titanite and zircon) are also prevalent.

It is conspicuous that mafic minerals (clinopyroxene, blue and green amphiboles, biotite) tend to occur in different types of clots comprising multiple grains of either identical or disparate ferromagnesian phases, accompanied by minor amounts of feldspars, quartz, accessory and opaque minerals (Figs 4 and 7–9; Table 2). The aggregated crystals are either completely intact or exhibit different stages of alteration. The number of single mafic minerals occurring in the groundmass varies from sample to sample, however, it is rather limited.

Clots associated with mafic microgranular enclaves have not been identified; however, certain varieties can be unequivocally attributed to metamorphic country rock xenoliths (Fig. 7E, F)

The type, the amount and the form of appearance of the ferromagnesian mineral assemblages could provide important information on the evolution of the encircling felsic rocks and may guide us to better understand their genesis. Thus, rather than describing the mineralogical and textural features of the different host rocks in detail, in the following subsections we will focus on the petrographic characteristics of the distinct mafic phases. It must be elucidated beforehand that the phrase "groundmass" is applied to the phaneritic, holocrystalline, predominantly felsic mineral-rich domain of the so-called "host rock" enclosing mafic aggregates.

Based on their characteristic petrographic features (e.g., type and texture of the main ferromagnesian components), clusters can be classified into the following characteristic groups (Fig. 4; Table 2).

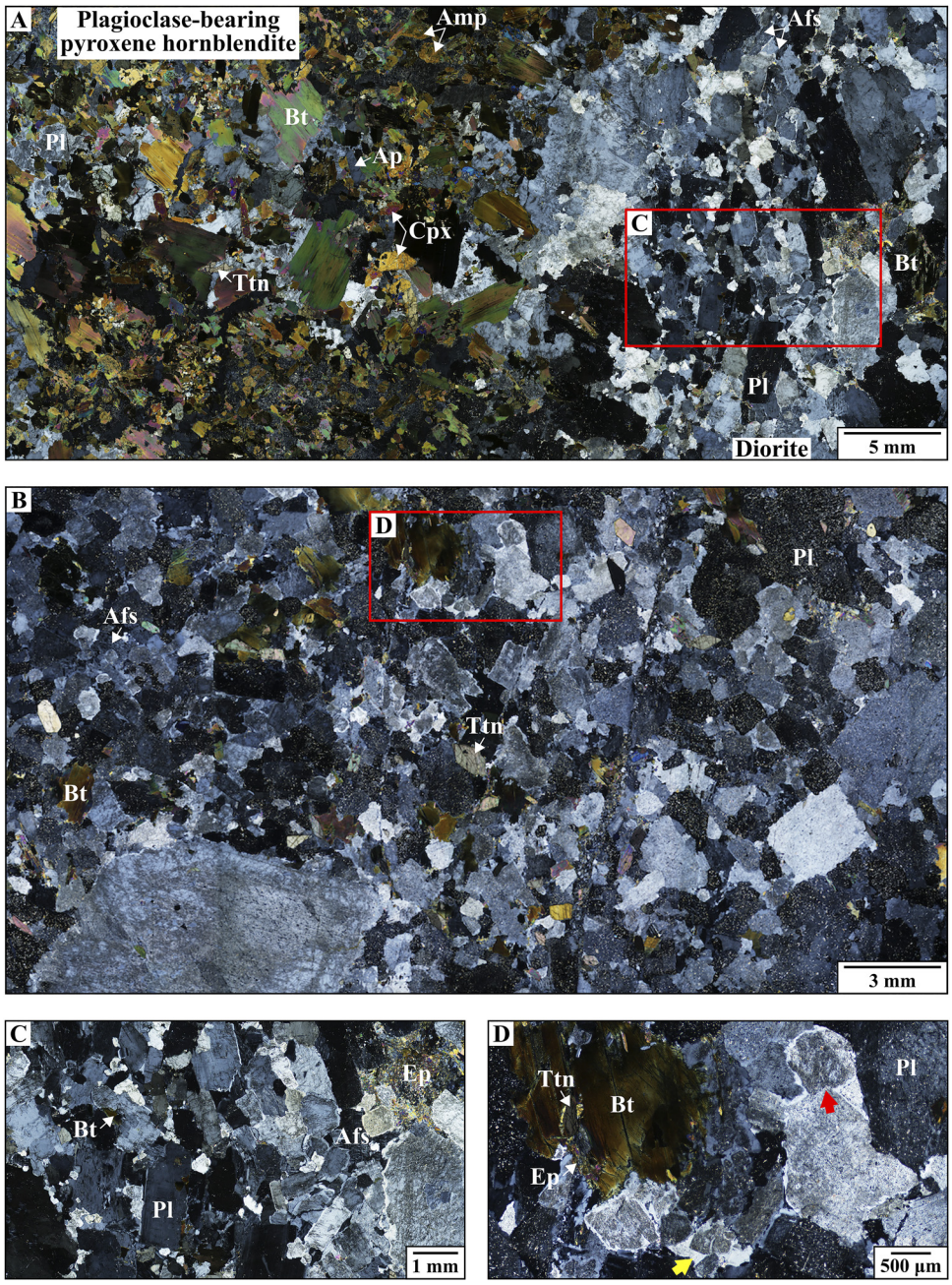

Fig. 6. Characteristic textural features of the studied felsic rocks belonging to Group 1. (A) Continuous transition between plagioclase-bearing pyroxene hornblendite and the mostly idiomorphic plagioclase-dominated diorite. The latter exhibits an oriented texture, +N (crossed polars). (B) Diorite containing disseminated biotite and feldspar megacrysts, +N. Note the straight crystal faces of touching plagioclases. (C) Aggregate of multiple feldspar grains with straight crystal faces in parallel orientation, +N. (D) Two impinged plagioclase crystals (marked by the red arrow) with separate cores. The yellow arrow is pointing at a cluster of multiple, sericitized and molded cores mantled by a pure rim, +N. Abbreviations of rock-forming minerals are after Whitney and Evans (2010)

Monomineralic mafic clots

Green amphibole-rich aggregate (abbreviated as G-Amp). These clusters comprise multiple crystals of intact green amphibole (magnesiohastingsite, determined by Raman spectroscopy) (Fig. 7A, B; Table 2). If zoned, a brown core is surrounded by a green rim. Amphibole might contain idiomorphic–hypidiomorphic apatite (Fig. 12A), titanite and occasionally opaque or zircon inclusions. Titanite and opaque grains are present either in the intergranular space between amphibole crystals or along the outer rim of the aggregates (Fig. 7A, B). In certain monzonite and monzogranite samples, the groundmass contains less intact actinolitic amphibole and it also appears in some of the *G-Amp* clots. In case the host rock exhibits oriented texture, amphiboles are aligned with their long axes parallel to the foliation. Thus, both the clusters and the minerals in them are oriented (Fig. 7B). Otherwise, randomly-aligned crystals

Table 2. Type, distinctive features and mineral assemblage of the mafic aggregates occurring in the felsic rocks of the Ditrău Alkaline Massif

Clot type		Sample	Size of the clots (mm)	Shape of the clots	Oriented texture	Modal proportion in the host (V/V%)	Grain-size of the host (mm)	Clot-forming minerals (appearance, size [mm] and modal proportion in the aggregates [V/V%])								
								Cpx	G-Amp	Act	B-Amp	Bt	Ep	Ttn	Opq	Pl
Monomineralic	**G-Amp**	LBH2 LI18 LTa29 LTo35 LTo37 LO43/2	0.6–6 max. 8		If the host has oriented texture	0.6–13	0.2–4		I–H 0.1–4	± H–X 0.2–1				± IG or RC	± IG or RC	± IG
	B-Amp	LO43/1 LO44	1–5			2–3	0.3–3	± H–X (moderately altered) 0.1–0.5 amorphous–prismatic (uralitic pseudomorphs) 0.3–2			I–X 0.1–3					
	Bt-Xen	LBH55/1 LBH55/2	2 (width), armouring the xenolith		Parallel to the foliation of the host		max. 0.5 (adjacent to the selvedge); max. 2 (away from the xenolith)					I–H 0.1–2		± IG		
	Bt-Dom	LHH23/1	0.6–4 (wispy bands: 0.8–3)	Some are subspherical	In wispy bands	18	0.1–1					I–H 0.1–2 (in clots); 0.08–0.3 (in wispy bands)			± RBt	± IG
	Bt-Ran	LHH23/2 LS25 LTo32 LTo35 LTo37 LO46 LO47 LO48 LO51 LBH55/1 LBH55/2 LBH56	0.4–4	Isometric or elongated		0.2–2 max. 5	0.1–3					I–H 0.1–2			± RBt	± IG
	Ep	LBH3 LBH4 LB12 LB14 LTa29 LBH55/1 LBH55/2	0.4–3	Amorphous, isometric or stubby to slightly elongated prismatic	If the host has oriented texture	0.1–6	0.1–2 max. 3						I–X 0.03–1			

(continued)

Table 2. Continued

Clot type		Sample	Size of the clots (mm)	Shape of the clots	Oriented texture	Modal proportion in the host (V/V%)	Grain-size of the host (mm)	Clot-forming minerals (appearance, size [mm] and modal proportion in the aggregates [V/V%])								
								Cpx	G-Amp	Act	B-Amp	Bt	Ep	Ttn	Opq	Pl
Polymineralic	**G-AmpBt**	LBH2 LI18 LS25 LS28 LTa29 LTo32 LTo35 LO43/2	1–3 max. 5	Isometric or stubby to moderately elongated prismatic	If the host has oriented texture	1–6	0.2–3		I–X 0.1–3 39–70	± H–X 0.3–2 max. 17		I–X 0.1–2 30–59		± IG I–X 0.1–0.9 max. 7	± IG	± IG
	B-AmpBt	LO44	2–4	Amorphous or stubby prismatic		0.8	0.3–3				H–X 0.2–2 93	H 0.8–2 7				
	AmpCpxTtnOpqBt	LTa29	5	Stubby to slightly elongated		2	0.2–2 (megacrysts: max. 5)	H–X 0.5–1 11	H 0.05–2 42	H–X 0.07–1 (inclusions in G-Amp); max. 0.6 (patches) 42		± IG	± IG	IG I–H 0.1–1 5	IG	± IG

Abbreviations: Cpx – clinopyroxene, G-Amp – green amphibole, Act – actinolite, B-Amp – blue amphibole, Bt – biotite, Ep – epidote, Ttn – titanite, Opq – opaque minerals, Pl – plagioclase; I – idiomorphic, H – hypidiomorphic, X – xenomorphic; IG – intergranular, RC – along the rims of the clot, RBt – along the rims of biotite. Clot name abbreviations can be found in the text

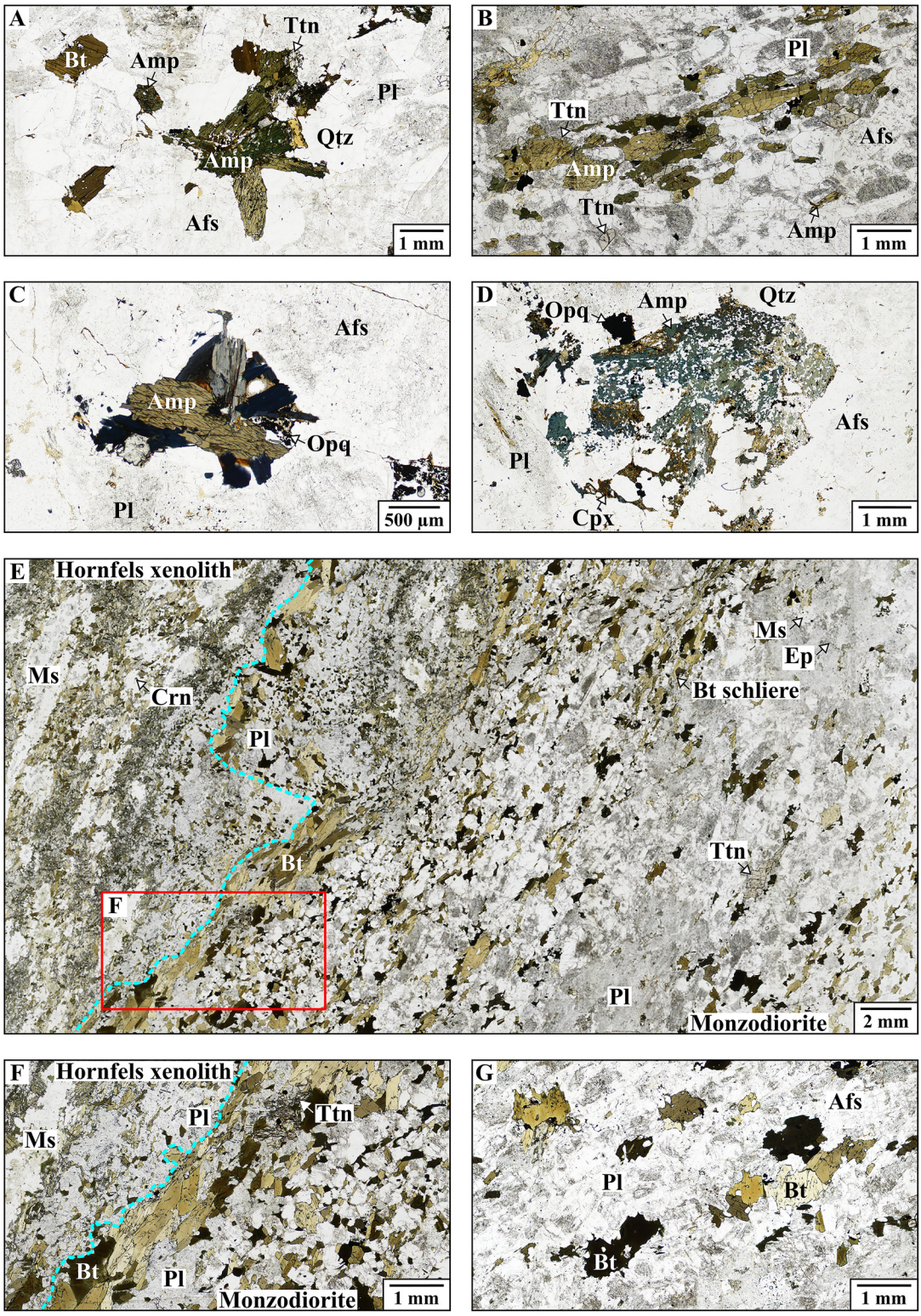

Fig. 7. Characteristic textural features of the monomineralic mafic clots occurring in felsic rocks of Group 2. (A) *G-Amp* aggregate adjoined by isolated amphibole and biotite, 1N (plane polarized light). (B) Elongated *G-Amp* clump exhibiting oriented texture, 1N. (C) *B-Amp* cluster, 1N. (D) *B-Amp* clot comprising spongy blue amphibole with minor clinopyroxene, 1N. (E) Biotite-rich selvedge (*Bt-Xen*) along the contact of the hornfels xenolith and the monzodiorite host rock, 1N. (F) Texture of the enclosing rock in the proximity of the biotite-dominated fringe (*Bt-Xen*), 1N. (G) Aggregated and isolated groundmass biotite in the monzodiorite host further away from the hornfels xenolith, 1N. Abbreviations of rock-forming minerals are after Whitney and Evans (2010)

make up the clumps. Isolated amphibole crystals have similar color and habit related to their aggregated counterparts (Fig. 7A, B).

Blue amphibole-rich aggregate (B-Amp). Randomly oriented blue amphibole (riebeckite) crystals make up these clots (Fig. 7C, D; Table 2). Most of the grains are entirely intact (Fig. 7C), whereas others exhibit a spongy texture due to numerous feldspar inclusions (Fig. 7D). Idiomorphic apatite, idiomorphic–hypidiomorphic opaque minerals and hypidiomorphic zircon are encircled by blue amphibole.

Although it is not prevalent, a few of the clusters contain moderately decomposed clinopyroxene (aegirine) (Fig. 7D). Amorphous masses as well as prismatic uralitic pseudomorphs after clinopyroxene are present in some of the clumps.

The amount of individually occurring blue amphibole is limited and some of them also show a spongy fabric. Scarce, isolated clinopyroxene may be present in the groundmass.

Biotite-rich aggregate (Bt). Based on their spatial distribution, three subtypes of *Bt* clumps can be distinguished: (1) metamorphic country rock xenolith-related clots, (2) clusters occurring in distinct domains of the enclosing rock and (3) randomly dispersed aggregates (Fig. 4).

Metamorphic country rock xenolith-related biotite-rich aggregate (Bt-Xen). This clot type is spatially associated with an approximately 20 cm long, ellipsoidal hornfels xenolith that becomes flattened toward its edges (Figs 3F and 7E, F). It is strongly decomposed and comprises profoundly sericitized plagioclase, – mostly aggregated – intact biotite blades and plates as well as masses of xenomorphic biotite intergrown with epidote. There are bands and almost isometric clumps of randomly-oriented muscovite flakes, some of which enclose xenomorphic remnants of corundum (Fig. 7E).

The hornfels xenolith is armored by an up to 2 mm wide, discontinuous selvedge (also known as selvage) of moderately to strongly elongated (± minor amount of equant) biotite (Fig. 7E, F; Table 2). Sagenitic biotite is also present in minor amount. Inclusions of biotite are represented by idiomorphic apatite, idiomorphic–hypidiomorphic titanite and hypidiomorphic zircon. Titanite also occurs in the intergranular space between biotite crystals (Fig. 7F). In the proximity of the xenolith, biotite of akin properties makes up intermittent mafic bands (schlieren) (Fig. 7E).

Aggregated biotite crystals have straight grain boundaries and either exhibit a shape-preferred orientation (aligned parallel to their long axes and to the orientation of the selvedge and schlieren as well) or lie at high angles to the main foliation (resembling a herringbone pattern) (Fig. 7E, F). These mafic bands follow the outline of the xenolith and are aligned parallel to the foliation of the enclosing rock.

Adjacent to the selvedge, the plagioclase-dominated monzodiorite host exhibits a honeycomb-like, fine-grained texture with interstitial biotite (Fig. 7E, F). Further away from the xenolith, the host rock progressively passes into a coarser-grained, oriented texture with more abundant alkaline feldspar. In this domain, clots of equant to strongly elongated, randomly or crystal face-parallel aligned biotite occur (Fig. 7G); however, mafic schlieren are totally absent. Isolated grains of equidimensional to slightly elongated platy biotite are also common and are aligned parallel to the foliation of the rock (Fig. 7G). Some of the aggregated and isolated groundmass biotite are embayed by feldspar grains.

Biotite-rich aggregate in distinct domains of the host rock (Bt-Dom). Clots of this group are concentrated into certain domains of the monzonite host. There are other areas in the enclosing rock that are entirely devoid of mafic minerals, whereas further zones contain exclusively isolated biotite crystals (Fig. 8A).

Equant to slightly elongated biotite makes up this clump type (Fig. 8A–C; Table 2). Idiomorphic zircon and hypidiomorphic–xenomorphic opaque minerals occur as inclusions. Opaque phases might also be present along the cleavage planes and rims of certain biotite grains (Figs 8B, C and 12B). Biotite flakes are either randomly oriented or aligned parallel to their crystal faces.

Occasionally, cluster-forming biotite becomes elongated toward the edge of the aggregate. These crystals are accompanied by more prolonged and smaller-sized biotite blades (± mostly equant feldspar and opaque phases); hence, some of the clumps are connected by these sinuous, wispy bands. In places, these aggregates of elongated biotite grains can be as narrow as a single crystal. Orientation of the prolonged grains (and most of the slightly elongated clot-forming biotite) coincides with the direction of the mafic bands (Fig. 8B). A few of the blade-like biotite crystals are rimmed by microcrystalline muscovite. Some of the interconnected clusters resemble a subspherical shape (Fig. 8C).

Biotite in the host is of similar size and appearance as its aggregated counterparts. Its shape-preferred orientation is not as pronounced; thus, it defines a weak foliation that is parallel to the mafic bands (Fig. 8A, B). Some biotite crystals (both in the encircling rock and in the clots) are embayed by feldspars.

Randomly distributed biotite-rich aggregate (Bt-Ran). Clumps of this group consist of equant to moderately (and minor strongly) elongated biotite crystals (Fig. 8D; Table 2). Idiomorphic–hypidiomorphic apatite and zircon, along with hypidiomorphic–xenomorphic titanite and opaque minerals are the most common inclusions. In few instances, opaque phases are dispersed along the cleavage planes and rims of biotite plates. Touching biotite grains have straight crystal faces and are either aligned parallel to them or lie at an angle.

Single biotite of akin characteristics also occurs in the host. Isolated and clot-forming biotite crystals are occasionally embayed by feldspars. Scarce, isolated green or blue amphibole and clinopyroxene might be present in the groundmass as well.

Epidote-rich aggregate (Ep). The cluster-forming epidote grains are either randomly oriented or aligned parallel to their crystal faces (Fig. 8E). If the host exhibits oriented fabric, the long axis of the prolonged aggregates coincides with the direction of the foliation (Table 2).

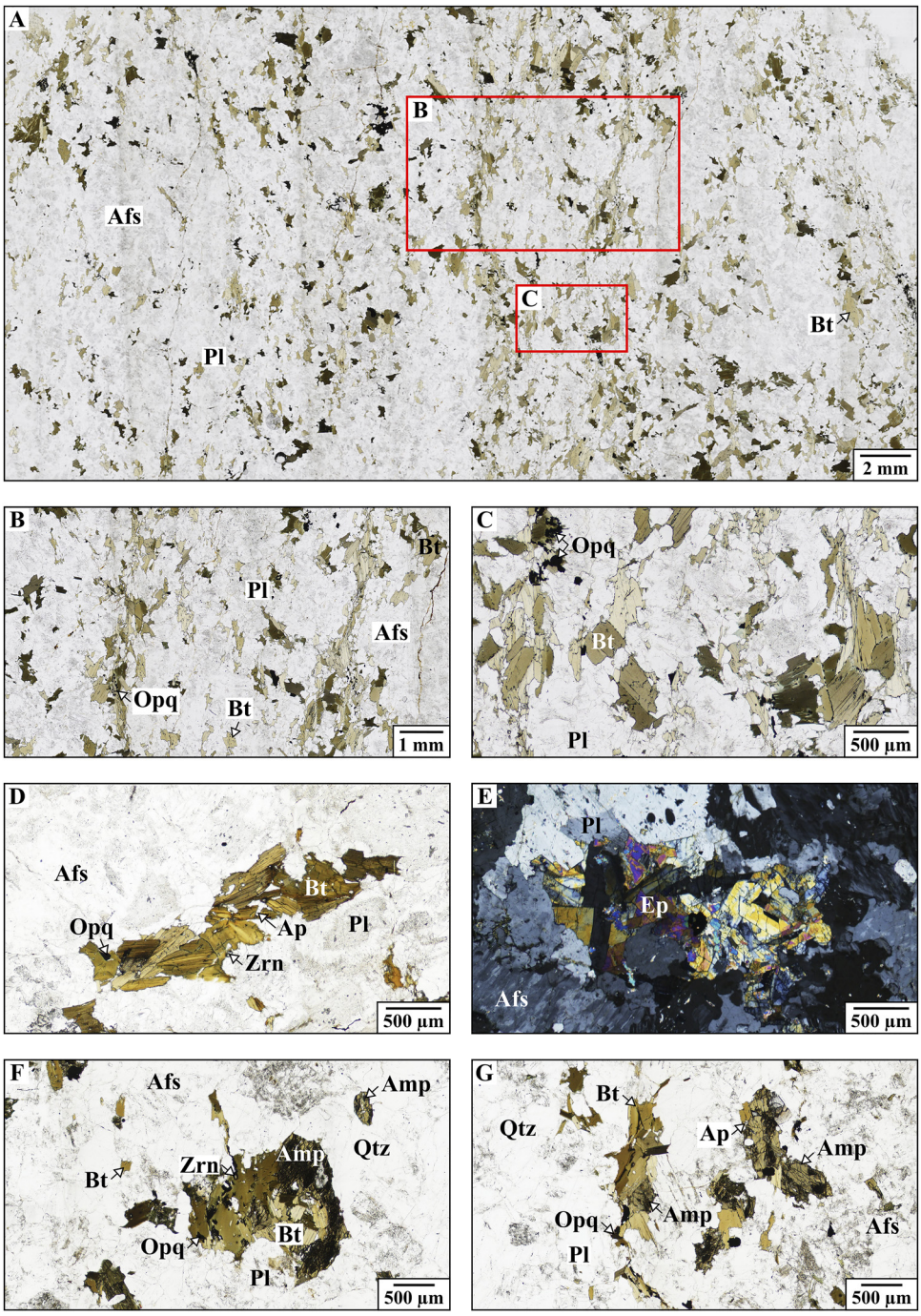

Fig. 8. Characteristic textural features of the monomineralic and polymineralic mafic clots in felsic rocks of Group 2. (A) *Bt-Dom* aggregates in distinct domains of the monzonite host, 1N (plane polarized light). (B) *Bt-Dom* clumps, interconnected by wispy bands made up of elongated blade-like biotite crystals, 1N. (C) Subspherical *Bt-Dom* cluster on the right side of the photomicrograph, 1N. (D) Slightly elongated, randomly distributed *Bt-Ran* clot, 1N. (E) *Ep* aggregate, +N (crossed polars). (F) Isometric *G-AmpBt* cluster adjoined by amphibole and biotite of the monzogranite host, 1N. (G) Elongated *G-AmpBt* clump, 1N. Abbreviations of rock-forming minerals are after Whitney and Evans (2010)

Apart from the clumps, epidote might be present as isolated crystals between the main rock-forming minerals or as inclusions within feldspars and biotite. It can also be intergrown with platy groundmass-biotite.

The host is either devoid of or contains minor amount of single green amphibole.

Polymineralic mafic clots

Green amphibole + biotite aggregate (G-AmpBt). Petrographic characteristics of this cluster type can be found in Table 2. Idiomorphic–hypidiomorphic apatite, titanite and zircon crystals are enclosed by green amphibole (Fig. 8F, G).

Isolated amphibole crystals might occur in the host rock as well.

Biotite (Fig. 8F, G) contains idiomorphic–hypidiomorphic apatite, titanite and zircon, along with hypidiomorphic–xenomorphic opaque inclusions (Fig. 12C). Single biotite plates of akin habit and optical properties may be present in the groundmass as well. Some of them as well as of the clot-forming biotite crystals exhibit a spongy fabric due to abundant feldspar inclusions. A single sample also includes scarce isolated blue amphibole.

Amorphous, isometric or prismatic aggregates of similar petrographic features, however, with altered versions of the comprising minerals, were also observed (Fig. 9A, B). There are other decomposed, isometric or prismatic clusters containing remnants of green amphibole (some of them have an actinolitic core), accompanied by chlorite, intact biotite flakes, titanite and opaque minerals (Fig. 9C, D). Isometric or prismatic clumps of altered as well as fresh biotite, titanite and opaque phases associated with minor muscovite and quartz occur in some of the samples (Fig. 9E). Clots of isometric or prismatic shape, comprising decomposed, along with intact biotite, epidote, titanite and opaque minerals were also found (Fig. 9F).

Blue amphibole + biotite aggregate (B-AmpBt). Petrographic features of this cluster type are summarized in Table 2. Aggregated blue amphibole (Fig. 9G) encloses idiomorphic apatite, idiomorphic–hypidiomorphic opaque and hypidiomorphic zircon crystals. Isolated blue amphibole is rarely present in the groundmass. Blue amphiboles of both the clumps and the host may exhibit spongy texture owing to abundant feldspar inclusions (Figs 9G and 12D).

Clot-forming biotite includes idiomorphic apatite, hypidiomorphic zircon and hypidiomorphic–xenomorphic opaque inclusions. The host rock contains minor single biotite. The amount of isolated clinopyroxene crystals is negligible.

Amorphous or prismatic aggregates of akin petrographic characteristics, albeit comprising altered versions of the cluster-forming phases, were also found (Fig. 9H). A reaction corona has developed around certain biotite flakes that are in contact with quartz grains of the groundmass. The peripheral area of such textures is composed of fine-grained blue amphibole and/or clinopyroxene, whereas the internal zone is made up of feldspars that are occasionally accompanied by opaque phases (Fig. 9H). There are other decomposed, prismatic clusters made up of altered, along with intact biotite, titanite, opaque minerals and clinopyroxene. The latter is present as inclusion enclosed by biotite, interstitially among the clot-forming biotite crystals as well as along the outline of the aggregates. In the case of the latter, the clinopyroxene rim occurs exclusively in places where the cluster-forming biotite is adjoined by quartz crystals of the syenogranite host rock (Fig. 9I).

Amphibole + clinopyroxene + titanite + opaque minerals ± biotite aggregate (AmpCpxTtnOpqBt). Amphibole is present in two distinct forms (Table 2). Magnesiohastingsite with cuspate boundaries (Fig. 9J) contains idiomorphic–hypidiomorphic apatite and titanite inclusions. The other variety, namely actinolite, is less intact and has a sieved or fibrous texture. It either occurs as numerous tabular or prismatic inclusions within magnesiohastingsite (and thus, producing a poikilitic fabric) or forms adjoining patches (Fig. 9J). The two amphibole types not only make up the clumps, but also occur as single grains in the monzonite host rock.

Pale brown as well as green clinopyroxene (augite, diopside) is present as crystal fragments (Figs 9J and 12E). In some aggregates, it is encircled by actinolite (Figs 9J and 12F). Isolated clinopyroxene is totally absent from the groundmass. Biotite occurs in very limited number in the host rock.

Other peculiar textural features of felsic rocks belonging to Group 2

Spongy mafic megacrysts. Idiomorphic–hypidiomorphic stubby to strongly elongated prismatic or columnar, occasionally chloritized, randomly distributed biotite megacrysts (up to 14 mm) occur in some of the host rocks. They exhibit spongy microtexture due to abundant feldspar inclusions (Fig. 10A).

Feldspar-rich aggregate (Fsp). Not only rocks of Group 1 but also many mafic clot-bearing rocks include clusters of multiple, idiomorphic–hypidiomorphic feldspar crystals that are aligned parallel to their crystal faces and have a separate, sericitized, sieve-textured and/or inclusion-laden core rimmed by an inclusion-free zone (Fig. 10B, C, marked by the red dashed lines). Some of the feldspar grains in contact exhibit a truncated zoning pattern due to the embayment of one crystal in another. Aggregates of plagioclase crystals also occur as inclusions within groundmass microcline (Fig. 10C, D, highlighted by red and purple dashed lines, respectively).

Feldspar megacrysts. Idiomorphic–hypidiomorphic alkaline feldspar (orthoclase and microcline) megacrysts (up to 11 mm) appear in the host rocks. Many of them enclose several fine-grained, idiomorphic–hypidiomorphic plagioclase crystals with a separate, sericitized, sieve-textured core mantled by a fresh rim. Plagioclase inclusions are either randomly oriented or are aligned parallel to the crystal faces of the host-mineral. Aggregates of multiple plagioclase grains encircled by alkaline feldspar megacrysts are also common (Fig. 10E, distinguished by red and purple dashed lines, respectively).

Likewise, the (alkaline feldspar) syenite dykes include copious idiomorphic–hypidiomorphic, tabular or columnar, randomly or slightly oriented alkaline feldspar (orthoclase and microcline) megacrysts (Fig. 10F, highlighted by purple dashed lines). Their size varies between 1 and 4 mm, nevertheless, some of them may reach 8 mm.

Adjacent feldspar crystals with different zoning sequences. The most common zonation pattern of feldspars is represented by a sericitized, sieve-textured, occasionally resorbed core, mantled by an inclusion-free rim (Figs 10B–E and 12G). Rarely, some crystals exhibit complex zoning and the clear rim is succeeded by another sericitized, sieve-

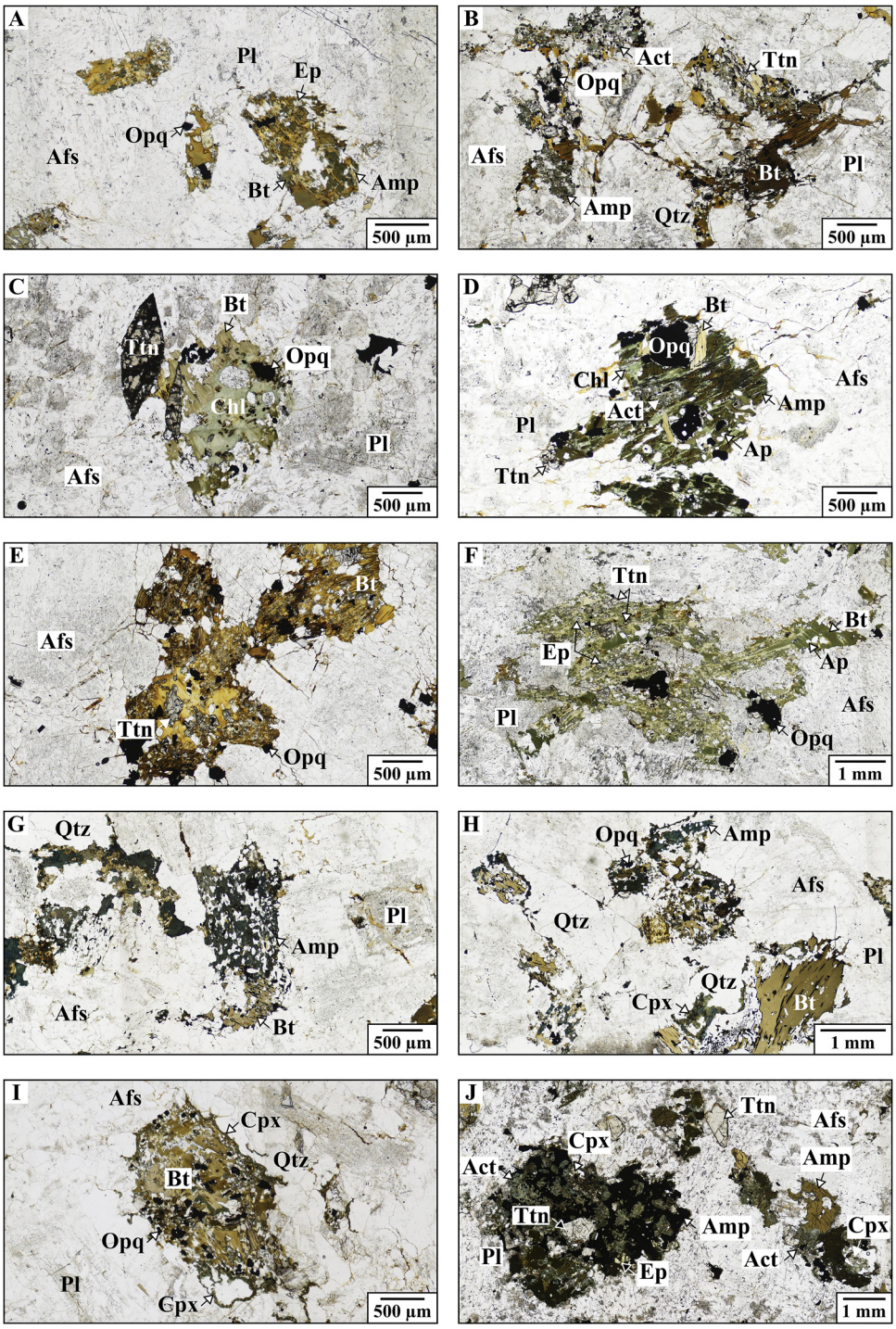

Fig. 9. Characteristic textural features of the polymineralic as well as of the altered mafic clots in felsic rocks of Group 2. (A) and (B) Altered clusters composed of green amphibole, biotite, titanite and opaque minerals with (B) containing additional actinolite, 1N (plane polarized light). (C) and (D) Altered clots comprising chlorite, biotite, titanite and opaque minerals with (D) including additional green amphibole with an actinolitic core, 1N. (E) Aggregate of decomposed biotite, titanite, opaque minerals accompanied by minor muscovite and quartz, 1N. (F) Clump containing decomposed biotite, epidote, titanite and opaque minerals, 1N. (G) Polymineralic *B-AmpBt* aggregate, 1N. Note the spongy fabric of blue amphibole. (H) Decomposed clusters of blue amphibole, biotite and clinopyroxene, 1N. Note the presence of a reaction corona in places where biotite is in contact with quartz crystals of the quartz syenite host. (I) Clot composed of altered biotite, clinopyroxene, titanite and opaque minerals, 1N. Note that clinopyroxene occurs along the periphery of the cluster where biotite is adjoined by quartz crystals of the syenogranite host. (J) Polymineralic *AmpCpxTtnOpqBt* clumps, 1N. Note the two clinopyroxene types (brown and green) occurring in the distinct clots. Abbreviations of rock-forming minerals are after Whitney and Evans (2010)

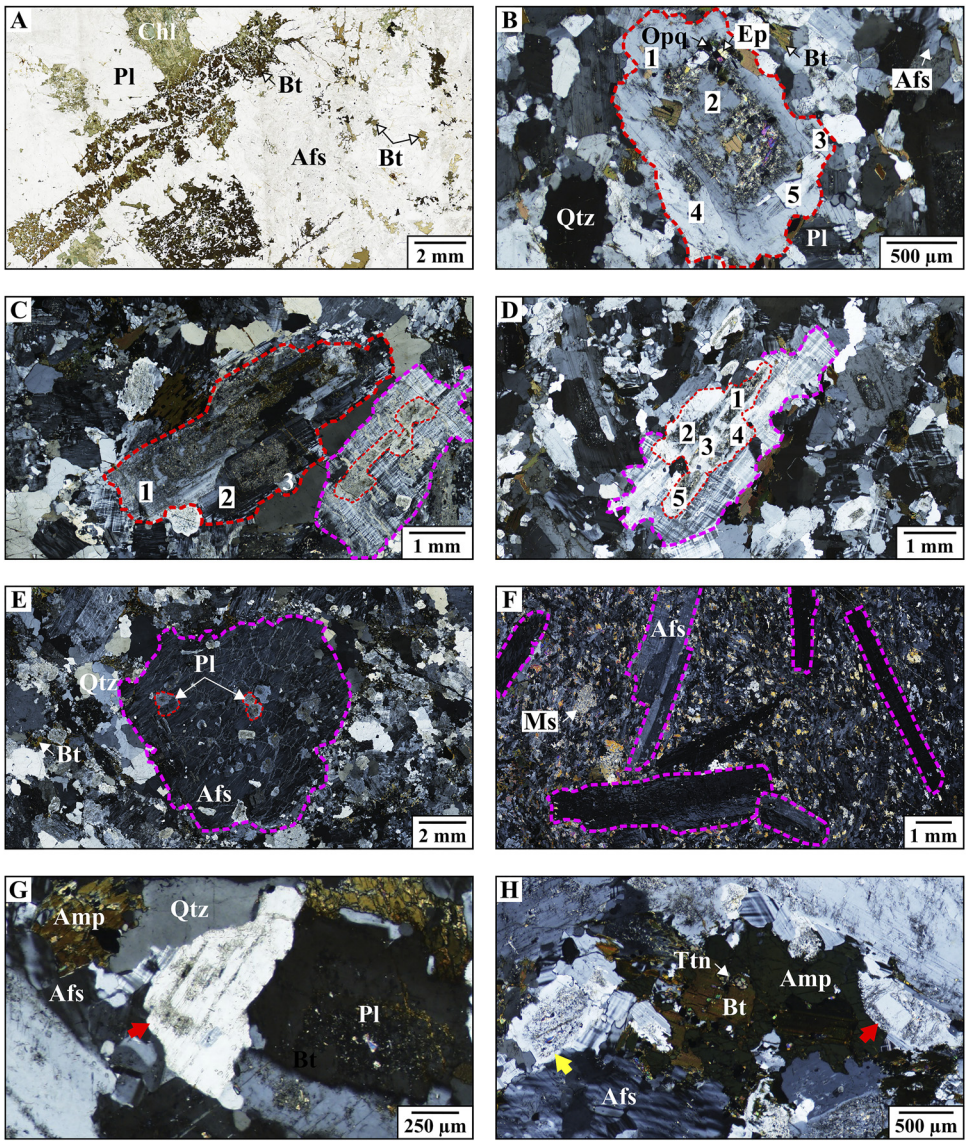

Fig. 10. Other peculiar features of the felsic rocks of Group 2. (A) Spongy biotite megacrysts, 1N (plane polarized light). (B) and (C) *Fsp* clusters (highlighted by red dashed lines) consisting of multiple grains (numbered) with separate cores in parallel orientation with (C) containing additional microcline (marked by purple dashed line) with plagioclase inclusions in synneusis relation (highlighted by red dashed line), +N (crossed polars). (D) Microcline (distinguished by purple dashed line) encircling plagioclase crystals (numbered and highlighted by red dashed line) in synneusis orientation, +N. (E) Alkaline feldspar megacryst (marked by purple dashed line) enclosing several separate or aggregated (highlighted by red dashed line) plagioclase grains with a sericitized, sieve-textured core, +N. (F) Slightly oriented alkaline feldspar megacrysts (distinguished by purple dashed lines) in alkaline feldspar syenite dyke with oriented texture, 1N. (G) Multiple-zoned feldspar crystal (marked by the red arrow), +N. (H) Normal-zoned feldspar (marked by the yellow arrow) adjoined by a reverse-zoned crystal (marked by the red arrow), 1N. Note that the latter is spatially associated with a mafic clot. Abbreviations of rock-forming minerals are after Whitney and Evans (2010)

textured zone, armored by a pure rim (Figs 10G, marked by the red arrow and 12H).

In a monzonite sample, feldspar grains exhibiting reverse, multiple-zoning (Fig. 10H, marked by the red arrow) occur along with the more frequent, normal-zoned crystals (Fig. 10H, marked by the yellow arrow). In this case, an idiomorphic, fresh core is enclosed by a sericitized, sieve-textured sector, followed by a peripheral zone of different width where inclusions are absent (Figs 10H, marked by the red arrow and 12I). Conspicuously, these reverse-zoned crystals are spatially related to mafic clots (i.e., directly attached to the clusters or else, occurring in their proximity), namely to *G-AmpBt* aggregates.

Biotite clusters in the metamorphic country rock spatially associated with granite and in the incorporated xenoliths. Approximately 10 cm-sized, ellipsoidal, intact country rock xenoliths can be found along the contact of the granite and the metamorphic rocks of the Tulgheş Lithogroup (Fig. 3E). Xenoliths become narrow towards their edges and pass into utmost 800 µm-wide contact zone-parallel bands (Fig. 11A). Both the hornfels xenoliths and

the identical wall rock contain abundant idioblastic–hypidioblastic almandine garnet up to 600 µm (Fig. 11). Approximately 1 cm further away from the contact, max. 1 mm-sized garnets occur in the metamorphic country rock (Fig. 11A). Garnet crystals of the xenoliths are completely intact (Fig. 11B), whereas in the wall rock some of them exhibit a reaction texture with biotite.

Another special feature of both the hornfels xenoliths and country rock is the presence of 0.5–4 mm-sized, isometric or elongated aggregates of randomly oriented, idiomorphic–hypidiomorphic biotite laths and plates (up to 800 µm), along with minor anatase and relict garnet (the latter two occur exclusively in biotite clumps of the wall rock) (Figs 11 and 12J). Some of the biotite crystals are chloritized.

Not as abundant as the biotite-rich clusters, however, subspherical microcrystalline muscovite-rich clots (up to 800 µm) also appear in the metamorphic country rock (Fig. 11C).

DISCUSSION

Indications of felsic crystal accumulation and other dynamic magma chamber processes from the Ditrău Alkaline Massif

The studied felsic suite of the DAM is considerably more diverse than previously thought. The heterogeneities are

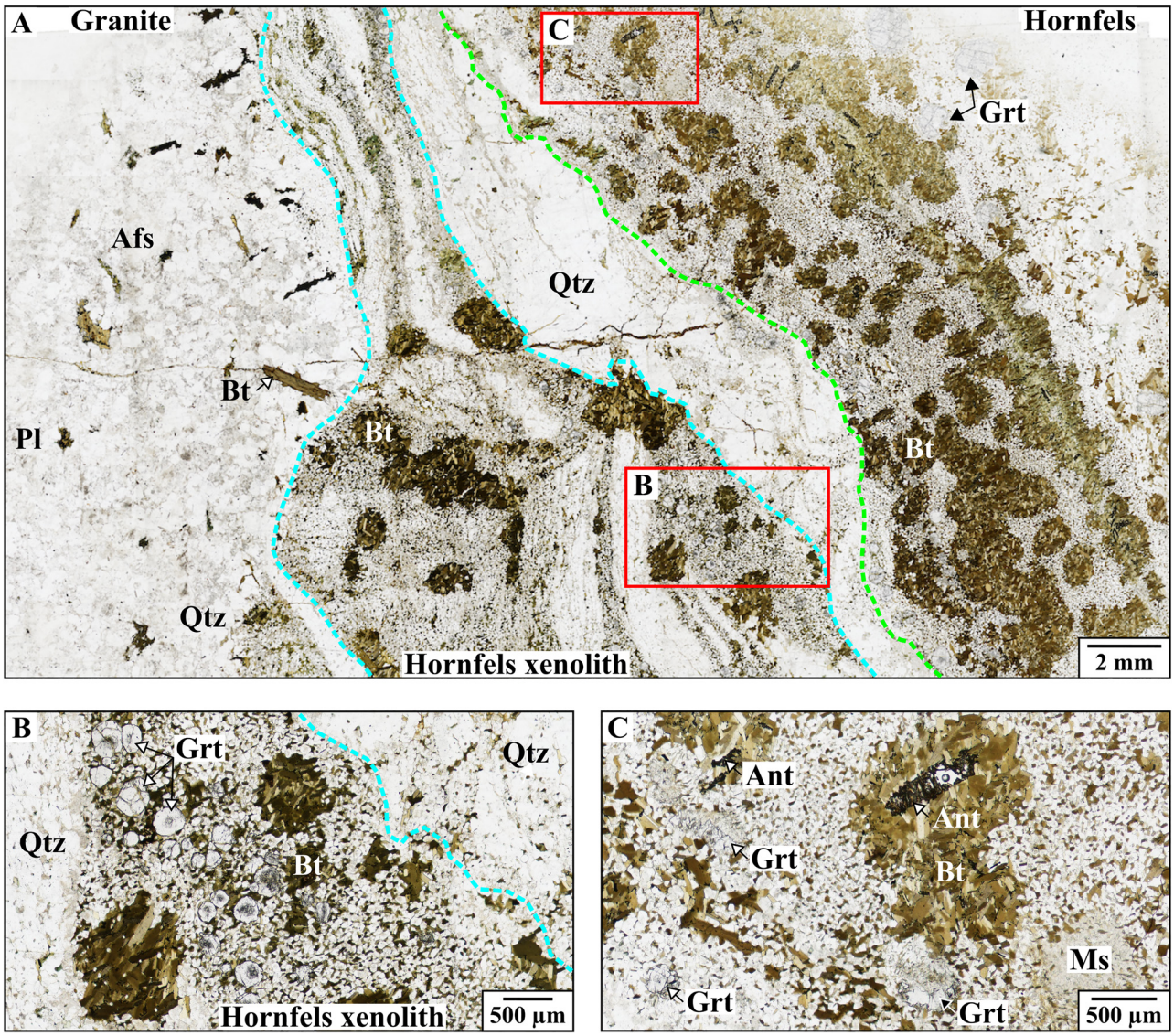

Fig. 11. Characteristic textural features of the hornfels wall rock and xenolith. (A) Contact of the granite and the hornfels country rock, 1N (plane polarized light). Note that the xenolith passes into a contact-zone parallel band. Margins of the xenolith are highlighted by turquoise, whereas the contact with the country rock is marked by green dashed lines. (B) Biotite-rich aggregates and garnet crystals of the metamorphic xenolith, 1N. Rim of the xenolith is distinguished by turquoise dashed line. (C) Anatase-bearing biotite-clots and a muscovite-dominated cluster of the metamorphic wall rock, 1N. Abbreviations of rock-forming minerals are after Whitney and Evans (2010)

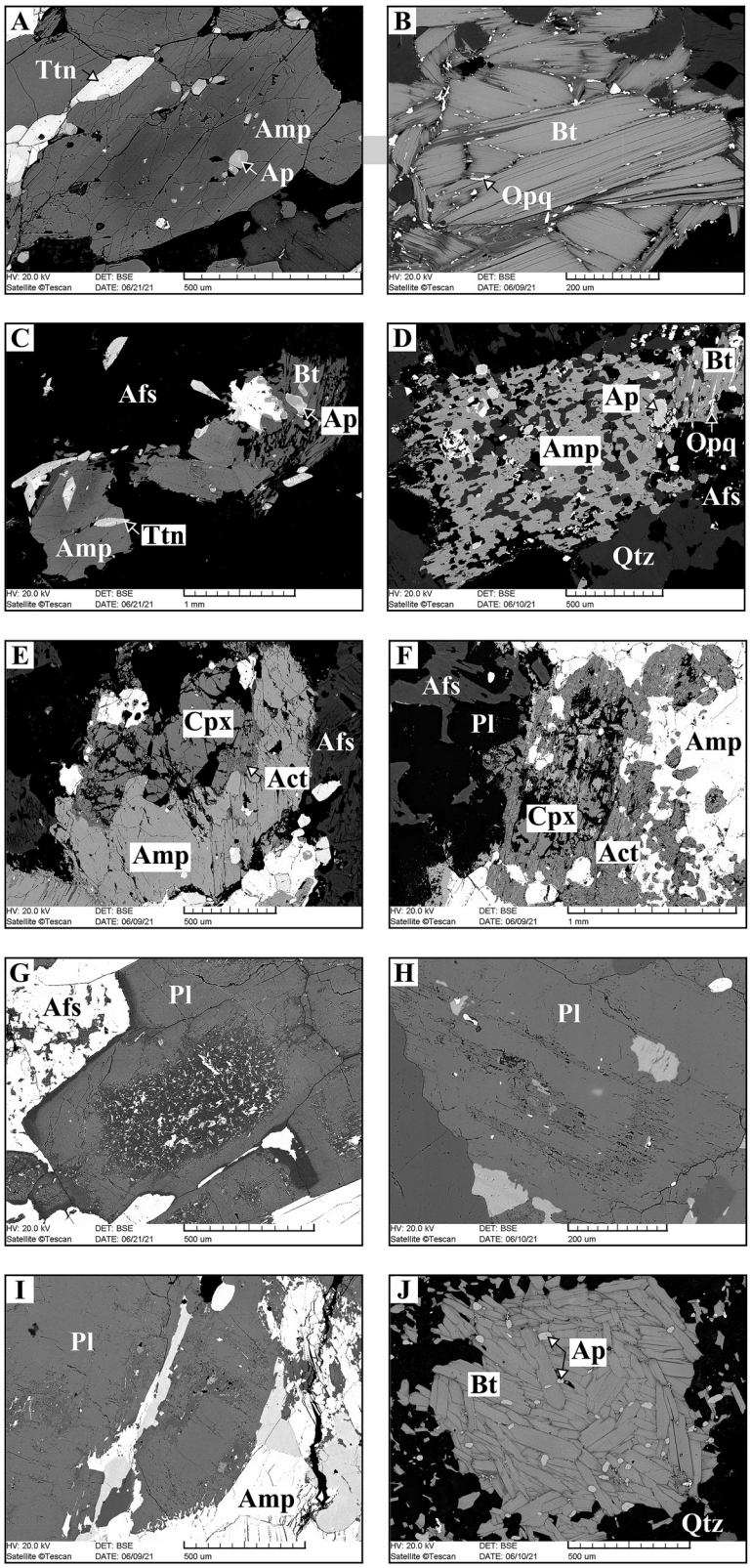

Fig. 12. SEM images of clot-forming ferromagnesian minerals and of felsic minerals in the groundmass. (A) Zoned green amphibole crystal with apatite inclusions in *G-Amp* aggregate. (B) Biotite plates rimmed by opaque minerals in *Bt-Dom* cluster. (C) *G-AmpBt* clot comprising both zoned and unzoned amphibole crystals. (D) *B-AmpBt* clump with spongy blue amphibole. (E) Green amphibole encircling clinopyroxene with minor actinolite in *AmpCpxTtnOpqBt* aggregate. (F) Actinolite surrounding clinopyroxene in *AmpCpxTtnOpqBt* cluster. (G) Typical zoning pattern of groundmass plagioclase with a sericitized core mantled by inclusion-free domains. (H) Multiple-zoned plagioclase exhibiting a sericitized core and zone. (I) Reverse-zoned plagioclase with a pure core encircled by a sericitized domain, followed by a rim where inclusions are absent. (J) Biotite-rich isometric clot in the hornfels xenolith. Abbreviations of rock-forming minerals are after Whitney and Evans (2010)

generally not of outcrop or macro-scale but rather occur at micro-scale.

Both types of felsic rocks (Group 1 and 2) contain abundant, idiomorphic–hypidiomorphic touching feldspar crystals that are aligned parallel to their crystal faces and define a shape-preferred orientation (Fig. 6A, C). If present, mafic minerals, clots and schlieren are also arranged accordingly (Fig. 7B, E, G). Such an arrangement results in strongly foliated igneous rocks, showing no sign of solid-state deformation. Feldspar lamination can either be attributed to gravity-driven compaction or to magmatic flow-induced shearing of the crystal mush (Vernon and Paterson, 2006 and references therein; Ildefonse and Fernandez, 1988; Féménias et al., 2005).

On a smaller scale, there are examples of aggregates embedded in the felsic groundmass comprising multiple feldspar crystals with a separate core and growth zones adhered in a parallel orientation (Fig. 10B, C). Furthermore, analogous clusters of smaller-sized plagioclase crystals occur as inclusions within alkaline feldspar of the felsic rocks (Fig. 10C, D) as well as in alkaline feldspar megacrysts (Fig. 10E). Such clumps are also known as "chain structure" (Vernon and Collins, 2011) and can be formed by a phenomenon Vogt (1921) described as "synneusis": suspended crystals may episodically drift together by turbulent currents (e.g., as a consequence of replenishment) or gravitational segregation (Brown, 1956; Brothers, 1964; Vance, 1969). Synneusis requires a high melt: crystal ratio; thus, it operates mostly in the early stages of crystallization. Based on these findings, feldspar crystals of such clusters – both in the groundmass and as inclusions – represent an earlier generation and may record turbulence due to either injection of new magma batch(es) (Vance, 1969) or to convection currents. Polycrystalline aggregates of felsic minerals are more capable of settling in viscous (felsic) magmas (Vernon and Collins, 2011) and abundance of such clots implies physical accumulation.

Some of the feldspars are embayed by another crystal (Fig. 6D, marked by the red arrow); nevertheless, clusters composed of multiple feldspar grains mutually impinging each other were also observed (Fig. 6D, marked by the yellow arrow). These crystals exhibit an irregular contact and a locally truncated zoning pattern. The embayed minerals have a separate, sericitized/sieve-textured core completely isolated by a few, continuous growth-zones. In most cases, crystals in such textural relation are mantled by a common, inclusion-free rim (Fig. 6D). Contact melting and embayment of the accumulated, touching crystals may be related to the compaction of the crystal mush (Park and Means, 1996; Vernon et al., 2004; Vernon and Collins, 2011). The pure rim is inferred to represent interstitial melts trapped among the accumulated crystals.

Different zonation of adjoining feldspars (Figs 10B–E, G, H and 12G–I) indicates distinctive crystallization and reaction histories. Zoning patterns of feldspars retained disequilibrium textures and thus, recorded evidences of dynamic magmatic events. Most of the feldspars show a common zonation: a sericitized/sieve-textured core is encircled by a pure rim (Figs 6C, D, 10B–E and 12G). This texture implies that significant changes occurred in the intensive variables (such as P, T or aH_2O) and/or in magma composition which could be related to the interaction with a more primitive magma. Bindea et al. (2020) interpreted the two-feldspar core-mantle textures (albite core rimmed by alkaline feldspar) as a resorption or replacement texture of a formerly-grown plagioclase by subsequent alkaline feldspar, amidst open-system magmatic circumstances.

Though not as abundant, there are some examples of feldspars exhibiting multiple (Figs 10G, marked by the red arrow and 12H) as well as reverse (Figs 10H, marked by the red arrow and 12I) zoning. In the first case, the core of the crystals is Ca-rich assumed by its profound sericitization. The core is mantled by a zone with a more sodic composition. It is followed by another domain of calcic spike which is armored by a Na-rich rim. The calcic core and zone might have originated from a magma of higher temperature and more mafic composition, whereas the sodic areas represent lower-temperature and relatively felsic environment. The different zones record the compositional changes in feldspars that can be attributed to variations in the magmatic conditions and thus, may imply multi-stage mixing events. Nevertheless, such multiple-zoned crystals are relatively scarce. Hence, it is more likely that their texture is the result of a smaller-scale/less-widespread process and indicates crystallization amidst fluctuating parameters (e.g., T and magma composition). Such conditions can easily be conceived during crystal transfer caused e.g., by turbulent currents. Turbulence is not necessarily independent of magma mixing/mingling; indeed, it is probable that single crystals of both end-members have been dragged by these currents during the invasion of the replenishing magma and became introduced into the new environment characterized by contrasting composition and intensive variables. Subsequent and repeated transport of single crystals from one magma into the other could have resulted in the observed textural features. Nevertheless, chamber-scale convection currents may also carry crystals and circulate them between various domains of the magmatic system defined by different chemical composition, P and T. Based on the dimension of the zones with different texture, the transported feldspar crystals either had not spent much time in either environment before they were introduced into the other one or became notably resorbed in the new setting.

Similarly, reverse zoning of feldspars (Figs 10H and 12I) hints that such crystals originate from an environment of different temperature and/or composition and their particular textural characteristics were formed by crystal transfer and/or interaction between different magma batches (Wiebe, 1968; Baxter and Feely, 2002; Vernon and Paterson, 2006). Their intact, inclusion-free core implies more sodic composition. It is succeeded by a relatively wide, extensively sericitized zone of supposedly more Ca-rich chemical composition. Such crystals are mantled by a possibly sodic rim where inclusions are absent. The core may have originated from the felsic magma and later became introduced into another environment of higher temperature and/or

contrasting composition and – based on the dimension of the sericitized domain – spent there a relatively long time before being transported back into its original setting. The outer rim is likely to represent the felsic end-member. The observation that reverse-zoned feldspars are spatially associated with mafic clots further supports the hypothesis that (at least some of) the latter originate from other regions of the magma storage system and/or became introduced into their present setting by magma mixing/mingling. The presence of antecrysts and mantled xenocrysts adjoining their mantle-free equivalents can also be explained by the felsic cumulate hypothesis (Vernon and Collins, 2011).

Based on these observations, the evolution of the investigated felsic rocks was driven by multiple magma chamber processes. Textural features – implying settling of felsic minerals, magmatic flow, strain of the crystal mush, magma mixing/mingling as well as turbulent convection – reveal the dynamic conditions that prevailed in the magmatic system. Crystal accumulation and flow fabrics indicate the presence of heterogeneous domains within the chamber. The former was confined to areas where shear flow and/or convection was limited, whereas the latter occurred in active regions where melt was more abundant. Repeated injection of more primitive magma into the felsic crystal mush, interaction of the two end-members as well as replenishment-induced convection and stirring along with temperature and/or density gradient-driven currents also played a crucial role in the development of the observed features.

Mafic clots in the felsic suite of the Ditrău Alkaline Massif: origin and significance

Felsic rocks of Group 2 appear to be homogeneous at macroscale (Fig. 3A–D); however, their microtextural features indicate that – beside minor isolated ferromagnesian minerals – they comprise mafic aggregates of various petrographic characteristics (Figs 4 and 7–9; Table 2). The observation that such clots are present in practically all of the felsic rocks of Group 2 indicates that cluster-formation was a widespread and common mechanism. They make a considerable contribution to enhancing the mafic mineral content of the host rocks, since not all of the ferromagnesian phases are considered to be of primary, direct magmatic origin.

Synneusis is a generally accepted concept for the genesis of felsic (plagioclase, alkaline feldspar or quartz) clusters (Vance, 1969); nevertheless, according to Vernon and Collins (2011), mafic clots may be formed by the same process as well. However, it should be noted that mafic clumps could be the products of various alternative mechanisms, details of which will be discussed henceforth.

Carvalho et al. (2017) found that maficity of diatexite magmas can be significantly increased by the raft and grain-scale disaggregation of mafic schollen. Lavaure and Sawyer (2011) focused particularly on country rock xenoliths and they also found that dismemberment of these inclusions plays an important role in increasing the modal proportion of ferromagnesian minerals (especially biotite) in the host. Based on the results of Batki et al. (2018) open-system processes, such as magma mixing and mingling, crystal transfer as well as recycling was significant in the petrogenesis of some rock types of the DAM (e.g., diorite, ijolite, syenite, tinguaite). The study by Ódri et al. (2020) shed light on the contribution of 20–60% upper crustal material during the evolution of the felsic suite (syenite, quartz syenite, quartz monzonite, granite).

Keeping in mind the above-mentioned information, it is likely that at least some of the mafic clumps are composed of replacive minerals after a precursor phase. Comparing all observed aggregate types, one can notice a continuous transition from almost intact clot-forming crystals through partial to complete replacement (pseudomorphism). Thus, different clusters might represent distinct stages of substitution of the entrained materials. Some clump types are presumed to be of different origin. Identification of the processes prevailing in the magma storage system is rather challenging and it is assumed that a combination of multiple, complex mechanisms resulted in the formation of the observed features. Figure 13 is a schematic illustration of how the modal proportion of the ferromagnesian phases could have been modified during these processes.

It is supposed that the base of the magma chamber comprises a mafic cumulate pile that is overlain by a felsic crystal mush. This system is periodically replenished by magma batches of more primitive composition (Fig. 13/1).

Due to the movement of the host magma, coherent magmatic enclaves and isolated ferromagnesian minerals are formed by the disruption of the mafic dyke (Fig. 13/2). Owing to the interaction with the igneous body, metamorphic wall rock xenoliths and country rock-derived isolated crystals become introduced into the felsic crystal mush. Turbulent currents – induced either by the invasion of the replenishing magma or by thermal and/or density gradients – may drag and deposit mafic cumulus mineral aggregates in the felsic system (Fig. 13/2).

Flow of the felsic melt leads to the separation of plagioclase from biotite and of elongated biotite crystals from the equant ones. The latter are introduced into the low shear strain (plagioclase-dominated) zones (Fig. 13/3). Shearing also promotes the disaggregation of the entrained inclusions. Continuous erosion of the incorporated magmatic enclaves and metamorphic xenoliths reduces their dimensions, adds ferromagnesian minerals into the felsic host and thus, leads to the formation of swarms comprising mafic phases. This way, clinopyroxene- and amphibole-bearing short and wide schlieren develop along the edges of the magmatic enclaves. The mafic bands are parallel to the margins of the rafts (Fig. 13/3). This mechanism strongly increases the maficity of the felsic lithologies. Interaction between the host and the incorporated substances leads to progressive changes in the mineral assemblage of the latter. Following their incorporation into the felsic system, the exotic materials become extensively modified and their ferromagnesian constituents are systematically replaced by secondary minerals (Fig. 13/3). Isolated clinopyroxene crystals begin to be replaced by actinolite (Castro and

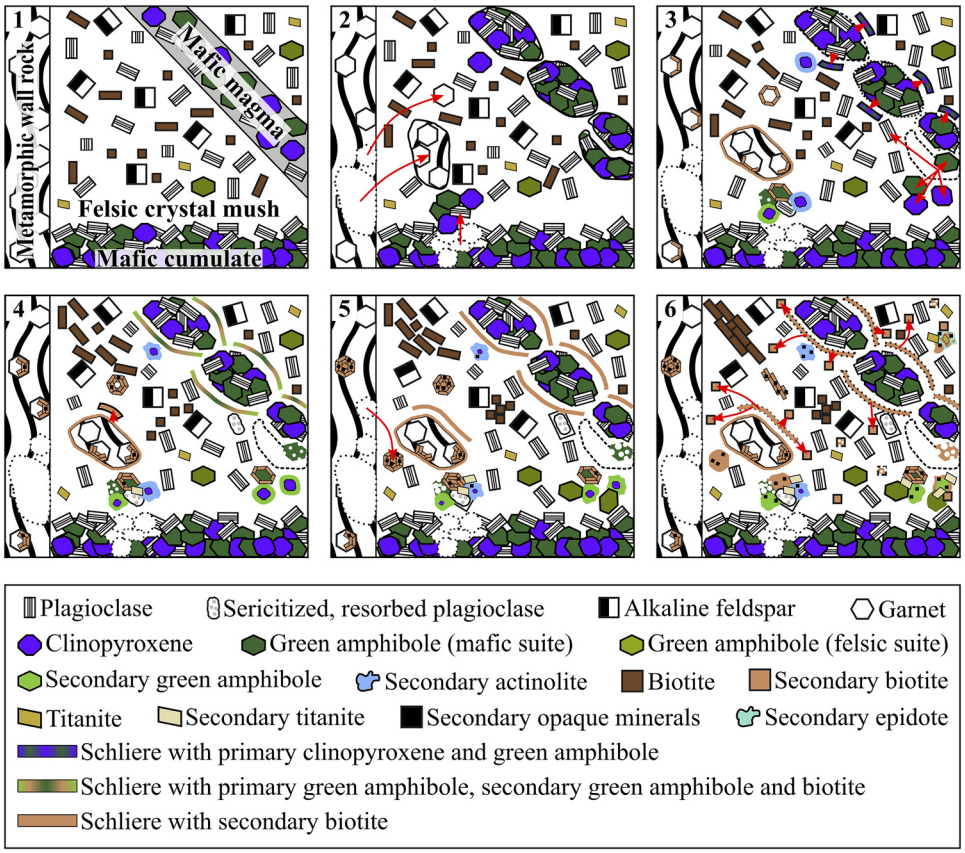

Fig. 13. Schematic interpretation of the processes involved in the formation of the studied mafic clots. Mechanisms associated with the development of felsic clots and cumulates are not represented for visual clarity. Relative size of the crystals and structural elements is not illustrated to scale. See text for details

Stephens, 1992). Garnet crystals are replaced by minor biotite (White et al., 2005) both in the mush and in the xenoliths. Due to the effect of the igneous body, replacive phases may develop in the metamorphic wall rock as well. Country rock xenoliths become completely mantled by a rim of biotite crystals (Fig. 13/3). *Bt-Xen* aggregate (Fig. 7E, F) can be interpreted as a selvedge formed along the interface of the metamorphic xenolith and the host magma due to chemical reaction between the two phases. K-content of the host may decrease due to the development of the biotite-dominated fringe. This phenomenon may have an effect on the amount of alkaline feldspar crystallizing from the melt (Kriegsman, 2001) and most possibly that is the reason why alkaline feldspar of the enclosing rock becomes more abundant further away from the enclave. Secondary green amphibole and actinolite, along with biotite are formed after clot-forming cumulus clinopyroxene and green amphibole, respectively. Some of the cumulate-derived amphiboles develop spongy texture implying they are not in equilibrium with their current setting (Fig. 13/3).

As the magmatic strain increases, schlieren containing minor primary green amphibole, along with secondary green amphibole and biotite after clinopyroxene and amphibole, respectively become elongated. Short and wide, biotite-rich schlieren become detached from the periphery of the metamorphic xenoliths. The primary incorporated minerals are further replaced by secondary phases (Fig. 13/4). Since clinopyroxene and amphibole can accommodate Ca, Y and REE in higher concentrations compared to biotite, the formation of secondary biotite after clinopyroxene or amphibole is accompanied by the crystallization of Ca-, Y- and REE-bearing accessory minerals (Ubide et al., 2014). This could account for the abundance of apatite, titanite, zircon and opaque phases occurring both in the interstices and on the margins of the studied clusters (e.g., Fig. 8D, F, G and Fig. 9D, J). Rims of exotic plagioclase become resorbed in the new environment characterized by different intensive variables and composition. Simultaneously, plagioclase crystals begin to be sericitized (Fig. 13/4).

Biotite completely replaces amphibole in the magmatic enclave-related schlieren (Fig. 13/5). Intact growth-zones develop around the resorbed and sericitized plagioclase cores. Xenolith-related biotite-rich schlieren become elongated. Some garnet crystals (both in the country rock and in the mush) are completely replaced by biotite, forming biotite-rich clumps and such pseudomorphs are further incorporated into the felsic system. Distribution of different minerals within the rock as well as extent of chemical potential gradient and diffusion coefficient bear a strong influence on the local reactions (Foster, 1986) and this could be the reason why pseudomorphs of garnet occur in the proximity of intact crystals (Figs 11 and 13). Equant biotite

crystals of the feldspar-rich domains form aggregates (Fig. 13/5). By this stage, the plagioclase-rich domain has attained the rigid percolation threshold and thus, the shear strain becomes more significant in the mafic mineral-rich bands. In the latter, biotite aggregates are formed initially, being followed by the imbrication of elongate crystals. New magmatic amphibole crystallizes on some of the secondary mineral-bearing clots (Fig. 13/5).

Schlieren are weaker than the feldspar-dominated host rock; hence, the postsub-magmatic strain is more pronounced in the mafic bands, which leads to the development of strongly elongated biotite-rich schlieren (Fig. 13/6). Development of *Bt-Dom* clots (Fig. 8A–C) could be explained by the heterogeneous mineral and shear strain distribution of the magma (Milord and Sawyer, 2003). In domains of higher magmatic strain, the biotite-rich aggregates formed after garnet also become elongated and form schlieren; otherwise, they retain the habit of the preceding crystal (Fig. 13/6). Schlieren-derived, detached biotite crystals become dispersed; thus, further increasing the maficity of the host. Actinolite and secondary biotite completely replace the isolated clinopyroxene and spongy green amphibole, respectively (Fig. 13/6), which implies that the latter were not in equilibrium with the melt. Flow of the host magma might completely disrupt the enclaves and xenoliths as well as the schlieren and then may thoroughly distribute the detached crystals (mostly biotite), developing a homogeneous texture in the host (Fig. 13/6). The formation of the opaque fringe and inclusions along the cleavage planes of biotite (Figs 8B, C and 12B) can be attributed to temperature-drop and/or deformation. Decreasing temperature, associated with chemical reaction between biotite and the trapped melt may result in the crystallization of a muscovite rim enveloping biotite as well as exsolution of opaque phases (Milord and Sawyer, 2003). Primary minerals of the clusters are either completely replaced (e.g., Fig. 8C, D) or are preserved as crystal relicts (e.g., Figs 8F, G and 9J). Complete substitution is inferred to be favored in melt-rich, more hydrous regions of the system. The replacive phases may recrystallize into a larger grain-size in order to decrease the surface area and energy and thus, attain greater stability (Fig. 13/6).

Some of the *G-AmpBt* aggregates (Fig. 8F, G) and *Bt-Ran* clusters (Fig. 8D) perfectly preserve the transition from intact green amphibole (Fig. 14/1), through biotite partially replacing and retaining the shape of amphibole (Fig. 14/2), along with biotite-dominated clumps containing minor amphibole (Fig. 14/3) to complete replacement by biotite and elongation of the clusters (Fig. 14/4).

Groundmass and clot-forming epidote (Fig. 8E) is most likely a hydrothermal, secondary phase that formed after amphibole and plagioclase (Bird and Spieler, 2004; Pandit et al., 2014; Kobylinski et al., 2020). Aggregates comprising decomposed mafic phases (Figs 9A–F, H, I and 13/6) are likely to be the products of post-magmatic processes (e.g., hydrothermal or deuteric alteration of primary ferromagnesian minerals and/or mafic clusters comprising intact crystals).

It should be noted that some of the ferromagnesian minerals defined as single mafic phases and considered as original, primary constituents of the felsic host rocks may not be related to their present enclosing rock, but were derived from the disaggregation of the exotic inclusions, clots and/or incorporation of single exotic crystals that have been thoroughly dispersed in the felsic system. This hypothesis is further supported by the fact that some of the isolated ferromagnesian minerals exhibit irregular grain boundaries

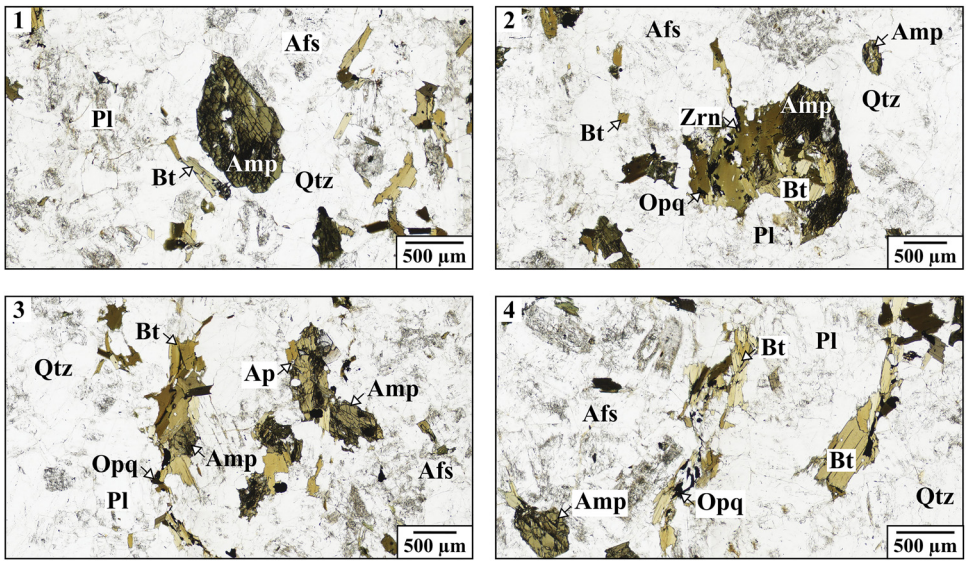

Fig. 14. Textural changes during the progressive interaction of incorporated green amphibole with the monzogranite host. (1) Hypidiomorphic, almost intact green amphibole in the host rock, 1N (plane polarized light). (2) Green amphibole partially replaced by biotite with accessory zircon and opaque minerals, 1N. (3) Stubby schliere comprising minor green amphibole and secondary biotite, 1N. (4) Elongated schlieren, made up of biotite with a well-developed shape-preferred orientation, completely replacing amphibole, 1N. Abbreviations of rock-forming minerals are after Whitney and Evans (2010)

as well as resorbed and spongy fabric, implying they are not in equilibrium with their current setting (Fig. 13/3–6).

The origin of isolated blue amphibole, along with different types of clusters containing blue amphibole (*B-Amp*, *B-AmpBt* and their altered versions) (Figs 7C, D and 9G, H and 12D) is rather puzzling. Riebeckite is a common, primary mineral in Na-rich alkaline igneous rocks (such as nepheline syenite, syenite, granite); nevertheless, it also occurs in crystalline schists as well as in rocks that were subjected to alkali metasomatism (e.g., fenitization) (Miyashiro, 1957; Nesse, 2017; Verschure and Maijer, 2005). The studied rocks containing single clinopyroxene, along with different types of blue amphibole-laden aggregates crop out in the proximity of nepheline syenite. Hence, some kind of relationship could be presumed between the clot-bearing rocks and nepheline syenite. Verschure and Maijer (2005) described replacement and corona textures identical to those of observed in the studied rocks (Fig. 9H). Such features can be interpreted as products of two-phase fenitization. In the first stage, breakdown of the original amphibole and biotite crystals had been initiated by the metasomatic process, leading to the formation of a reaction corona comprising Na-pyroxene and feldspars (Fig. 9I). It was followed by a second phase, where, among others, Na-amphibole replaced the formerly generated Na-pyroxene as well as primary amphibole and biotite (Fig. 9G, H). Na-metasomatism has previously been reported from the DAM e.g., by Streckeisen (1960), Streckeisen and Hunziker (1974), Jakab et al. (1987), Kräutner and Bindea (1998) as well as by Pál-Molnár (2000). Thus, it could be a plausible mechanism for forming the isolated blue amphiboles and blue amphibole-bearing clots.

Summarizing our observations, metamorphic country rock xenoliths can be traced along the border zone of the igneous body (Figs 2D and 3E, F and 7E, F and 11A, B); whereas, farther into the center of the pluton, schlieren are more characteristic and different types of mafic clusters are abundant (Figs 7A–D, 8 and 9). Metamorphic rocks enveloping the DAM as well as country rock xenoliths contain abundant garnet crystals that are accompanied by aggregates of randomly-oriented biotite laths and plates (Figs 11 and 12J). These clots are identical to that of the "biotite atolls" described by White et al. (2005) and they have been interpreted as pseudomorphs after garnet. Disaggregation of the enclaves, entrainment of garnet and subsequent replacement by biotite (Fig. 13/2–6) or alternatively, involvement of previously replaced grains (pseudomorphs) (Fig. 13/5–6) could account for (at least some of) the biotite-rich aggregates observed in the felsic rocks of the DAM.

The origin of the clots in the inner areas of the massif is less clear, since in most cases secondary minerals replace the primary ones; furthermore, the robust evidences of magma chamber processes have either been obliterated or cannot be observed due to the poor exposures. However, there are a few locations where proofs of open-system magmatic processes (e.g., magma mixing/mingling) can be investigated (e.g., Heincz et al., 2018). If such interaction was involved in the formation of the studied felsic suite and it occurred at the early stages of crystallization, the felsic and mafic end-members could have thoroughly mixed, leading to the complete homogenization of the mafic intrusion. Absence of mafic microgranular enclaves may be explained by this mechanism (Fernandez and Barbarin, 1991). With advanced crystallization of the felsic mush, hybridization of the mafic magma becomes progressively hindered and thus, magma mingling prevails. This process favors the formation of mafic enclaves. Such magma blobs can be distributed in the chamber; e.g., by large-scale convection currents. Enclaves are likely to be disaggregated during their transport or due to the movement of the host magma (Fernandez and Barbarin, 1991). This second hypothesis seems to be more feasible to interpret the lack of the aforementioned structural features, adding that the scarcity of outcrops could also prevent one from recognizing and investigating the magmatic enclaves. Thus, it is likely that some of the mafic aggregates occurring in the studied felsic rocks retain the vestiges of magma mixing/mingling event(s).

Assuming that dynamic conditions prevailed in the magma chamber, thermal and/or density gradient-related convection or replenishment-induced currents could have accounted for crystal/mush transfer and/or recycling that resulted in the formation of certain mafic clusters.

CONCLUDING REMARKS

The presence and combination of the observed microtextural features (e.g., feldspar clots, adjoining feldspars with different zoning sequences, mafic aggregates, metamorphic country rock xenoliths) infer that the studied felsic rocks of the Ditrău Alkaline Massif (Eastern Carpathians, Romania) crystallized under dynamic magmatic conditions. Such circumstances can easily be conceived in an open magma storage system periodically invaded by new magma batches. Interaction of the distinct magmas resulted in mixing and mingling event(s); furthermore, magmatic stirring was induced by the injection of the replenishing magma. Convection currents may have also developed as a consequence of thermal and/or density gradients. Heterogeneous domains are likely to have been formed within the chamber with regions of limited shear flow and/or convection. This environment favored the accumulation of felsic minerals. Magmatic flow and turbulent currents prevailed in the melt-rich domains.

Felsic rocks of Group 1 (occurring on the hillside west of the Bordea Creek) exhibit distinct textural features that are characteristic of felsic cumulates. Rocks that had previously been classified into different types might be interpreted as accumulations of felsic minerals in different proportion.

Felsic rocks belonging to Group 2 (exposed between the Teasc and the Rezu Mare Creeks) also bear traces of felsic crystal accumulation. Furthermore, they enclose different types of mafic aggregates. Mafic clots could have been formed by several mechanisms. However, based on their modal composition and textural features complemented by the results of former studies, some of the clusters are

potential polycrystalline pseudomorphs after antecrysts and/or xenocrysts that were incorporated either by interaction between different magma batches, crystal transfer/recycling and/or by wall rock contamination. Aggregates show different stages of replacement of the precursor phase(s). Certain biotite-rich clumps could have been formed by chemical reaction between the metamorphic wall rock xenoliths and the host as well as by heterogeneous distribution of shear strain in the crystal mush. Some of the clusters comprising decomposed mafic minerals could be related to late-stage or post-magmatic modification of the ferromagnesian phases and/or mafic aggregates.

Crystal accumulation, crystal transfer/recycling, magma mixing and mingling as well as incorporation of exotic materials cannot be proved by macroscopic and microscopic structural and textural features alone. Hence, recent data of the ongoing mineral-scale geochemical analyses will be applied to unravel the further details of the presumed open-system magmatic processes to understand more about the genesis of the felsic suite of the Ditrău Alkaline Massif.

ACKNOWLEDGEMENTS

LK is indebted to fellow PhD students, Emese Tóth, Máté Szemerédi and Péter Gál for their generous assistance and excellent company during their fieldwork and sampling. The authors are grateful to Sándor Józsa of Eötvös Loránd University, Budapest, Hungary for the careful preparation of thin sections. Kristóf Fehér of MTA-ELTE Volcanology Research Group, Budapest, Hungary is gratefully acknowledged for his assistance with SEM analyses. Thanks go to the staff of 'Vulcano' Petrology and Geochemistry Research Group, Department of Mineralogy, Geochemistry and Petrology, University of Szeged, Szeged, Hungary. The detailed review, constructive comments and helpful suggestions of Balázs Kiss (Institute of Geography and Earth Sciences, Eötvös Loránd University, Budapest, Hungary) and of an anonymous reviewer are highly appreciated and contributed to improve this article. Zsolt Benkó is gratefully acknowledged for his editorial work on the manuscript.

REFERENCES

Baker, D.R. (1996). Granitic melt viscosities and configurational entropy models for their calculations. *American Mineralogist*, 81: 126–134.

Baker, D.R. (1998). Granitic melt viscosity and dike formation. *Journal of Structural Geology*, 20: 1395–1404.

Balintoni, I. (1997). *Geotectonica terenurilor metamorfice din România*. Ed. Carpatica, Cluj Napoca, p. 176.

Balintoni, I., Balica, C., Ducea, H., and Horst-Peter, H. (2014). Peri-Gondwanan terranes in the Romanian Carpathians: a review of their spatial distribution, origin, provenance, and evolution. *Geoscience Frontiers*, 5(3), 395–411.

Balintoni, I., Gheuca, I., and Vodă, Al. (1983). Pânze de încălecare Alpine şi Hercinice din zona sudică şi centrală a Zonei Cristalino Mezozoice din Carpaţii Orientali. (Alpine and Hercynian overthrust nappes from central and southern areas of the East Carpathians Crystalline Mesozoic Zone). *Anuarul Instutului de Geologie şi Geofizică al României*, 60: 15–22.

Batki, A., Pál-Molnár, E., Dobosi, G., and Skelton, A. (2014). Petrogenetic significance of ocellar camptonite dykes in the Ditrău Alkaline Massif, Romania. *Lithos*, 200–201: 181–196.

Batki, A., Pál-Molnár, E., Jankovics, M.É., Kerr, A.C., Kiss, B., Markl, G., Heincz, A., and Harangi, Sz. (2018). Insights into the evolution of an alkaline magmatic system: an in situ trace element study of clinopyroxenes from the Ditrău Alkaline Massif, Romania. *Lithos*, 300–301: 51–71.

Baxter, S. and Feely, M. (2002). Magma mixing and mingling textures in granitoids: examples from the Galway granite, Connemara, Ireland. *Mineralogy and Petrology*, 76: 63–74.

Bea, F. (2010). Crystallization dynamics of granite magma chambers in the absence of regional stress: Multiphysics modeling with natural examples. *Journal of Petrology*, 51(7), 1541–1569.

Bindea, G., Nakano, S., and Makino, K. (2020). Multi-stage reorganizations of feldspars in felsic rocks of the Ditrău Alkaline Intrusive Complex, Romania. *Carpathian Journal of Earth and Environmental Sciences*, 15(2), 491–514.

Bird, D.K. and Spieler, A.R. (2004). Epidote in geothermal systems. *Reviews in Mineralogy and Geochemistry*, 56: 235–300.

Brothers, R.N. (1964). Petrofabric analyses of Rhum and Skaergaard layered rocks. *Journal of Petrology*, 6: 255–274.

Brown, G.M. (1956). The layered ultrabasic rocks of Rhum, Inner Hebrides *Philosophical Transactions of the Royal Society of London, Series B, Biological Sciences*, 240: 1–53.

Carvalho, B.B., Sawyer, E.W., and Janasi, V.A. (2017). Enhancing maficity of granitic magma during anatexis: entrainment of infertile mafic lithologies. *Journal of Petrology*, 58(7), 1333–1362.

Castro, A. and Stephens, W.E. (1992). Amphibole-rich polycrystalline clots in calc-alkaline granitic rocks and their enclaves. *Canadian Mineralogist*, 30: 1093–1112.

Chappell, B.W. (1978). Granitoids from the Moonbi district, New England Batholith, eastern Australia. *Journal of the Geological Society of Australia*, 25: 267–284.

Chappell, B.W., White, A.J.R., and Wyborn, D. (1987). The importance of residual source material (restite) in granite petrogenesis. *Journal of Petrology*, 28(6), 1111–1138.

Clemens, J.D., Petford, N., and Mawer, C.K. (1997). Ascent mechanisms of granitic magmas: Causes and consequences. In: Holness, M.B. (Ed.), *Deformation-enhanced fluid transport in the Earth's crust and mantle*. Mineralogical Society Series, Chapman and Hall, London, 8: 145–172.

Collins, W.J., Wiebe, R.A., Healy, B., and Richards, S.W. (2006). Replenishment, crystal accumulation and floor aggradation in the megacrystic Kameruka Suite, Australia. *Journal of Petrology*, 47: 2073–2104.

Didier, J. (1987). Contribution of enclave studies to the understanding of origin and evolution of granitic magmas. *Geologische Rundschau*, 76/1: 41–50.

Dingwell, D.B., Romano, C., and Hess, K.-U. (1996). The effect of water on the viscosity of a haplogranitic melt under P-T-X

conditions relevant to silicic volcanism. *Contributions to Mineralogy and Petrology*, 124: 19–28.

Dingwell, D.B., Scarfe, C.M., and Cronin, D.J. (1985). The effect of fluorine on viscosities in the system Na_2O–Al_2O_3–SiO_2: implications for phonolites, trachytes and rhyolites. *American Mineralogist*, 70: 80–87.

Féménias, O., Coussaert, N., Brassinnes, S., and Demaiffe, D. (2005). Emplacement processes and cooling history of layered cyclic unit II-7 from the Lovozero alkaline massif (Kola Peninsula, Russia). *Lithos*, 83: 371–393.

Fernandez, A.N. and Barbarin, B. (1991). Relative rheology of coeval mafic and felsic magmas: nature of resulting interaction process. Shape and mineral fabrics of mafic microgranular enclaves. In: Didier, J. and Barbarin, B. (Eds.), *Enclaves and Granite Petrology. Developments in Petrology*, Elsevier, Amsterdam, 13: 263–276.

Foster, C.T. (1986). Thermodynamic models of reactions involving garnet in a sillimanite/staurolite schist. *Mineralogical Magazine*, 50: 427–439.

Frost, T.P. and Mahood, G.A. (1987). Field, chemical and physical constraints on mafic-felsic interaction in the Lamarck Granodiorite, Sierra Nevada, California. *Geological Society of America Bulletin*, 99: 272–291.

Heincz, A., Pál-Molnár, E., Kiss, B., Batki, A., Almási, E.E., and Kiri, L. (2018). Nyílt rendszerű magmás folyamatok: magmakeveredés, kristálycsere, kumulátum recirkuláció nyomai a Ditrói Alkáli Masszívumban (Orotva, Románia). *Földtani Közlöny*, 148/2: 125–142.

Huang, X.-D., Lu, J.-J., Sizaret, S., Wang, R.-C., Wu, J.-W., and Ma, D.-S. (2018). Reworked restite enclave: petrographic and mineralogical constraints from the Tongshanling intrusion, nanling Range, South China. *Journal of Asian Earth Sciences*, 166: 1–18.

Hughes, C.J. (Ed.) (1982). *Igneous Petrology*. Developments in Petrology, Elsevier, Amsterdam, 7, p. 551.

Ildefonse, B. and Fernandez, A. (1988). Influence of the concentration of rigid markers in a viscous medium on the production of preferred orientations. An experimental contribution: 1. Non coaxial strain. *Bulletin of the Geological Institutions of the University of Uppsala*, 14: 55–60.

Jakab, Gy., Garbaşevschi, N., Balla, Z., Zakariás, L., Péter, J., Strungaru, T., Hereda, N., Sileanu, T., Aronescu, M., Postolache, C., Mocanu, V., Teulea, G., Hannich, D., and Tiepac, I. (1987). *Sinteza datelor obţinute prin prospecţiuni geologice complexe, lucrări miniere şi foraje, executate pentru minereuri de metale rare şi disperse, feroase şi neferoase în masivul de roci alcaline de la Ditrău, jud. Hargita. Arhiva IPEG, „Harghita"*, Miercurea-Ciuc, Manuscript.

Klaver, M., Matveev, S., Berndt, J., Lissenberg, C.J., and Vroon, P.Z. (2017). A mineral and cumulate perspective to magma differentiation at Nisyros volcano, Aegean arc. *Contributions to Mineralogy and Petrology*, 172: 95.

Kobylinski, C., Hattori, K., Smith, S., and Plouffe, A. (2020). Protracted magmatism and mineralized hydrothermal activity at the Gibraltar Porphyry copper-molybdenum deposit, British Columbia. *Economic Geology*, 115(5), 1119–1136.

Kräutner, H.G. and Bindea, G. (1995). The Ditrău alkaline intrusive complex and its geological environment. *Romanian Journal of Mineralogy*, 77/3: 1–44.

Kräutner, H.G. and Bindea, G. (1998). Timing of the Ditrău alkaline intrusive complex (Eastern Carpathians, Romania). *Slovak Geological Magazine*, 4: 213–221.

Kriegsman, L.M. (2001). Partial melting, partial melt extraction and partial back reaction in anatectic migmatites. *Lithos*, 56: 75–96.

Kumar, S. and Singh, R.N. (Eds) (2014). *Modelling of magmatic and allied processes*. Springer International Publishing, Switzerland, p. 246.

Lavaure, S. and Sawyer, E.W. (2011). Source of biotite in the Wuluma Pluton: replacement of ferromagnesian phases and disaggregation of enclaves and schlieren. *Lithos*, 125: 757–780.

Le Maitre, R.W., Streckeisen, A., Zanettin, B., Le Bas, M.J., Bonin, B., and Bateman, P. (Eds) (2002). *Igneous rocks: a classification and glossary of terms*. Cambridge University Press, Cambridge, p. 252.

Miller, C.F. and Miller, J.S. (2002). Contrasting stratified plutons exposed in tilt blocks, Eldorado Mountains, Colorado River Rift, NV, USA. *Lithos*, 61: 209–224.

Milord, I. and Sawyer, E.W. (2003). Schlieren formation in diatexite migmatite: examples from the St Malo migmatite terrane, France. *Journal of Metamorphic Geology*, 21: 347–362.

Miyashiro, A. (1957). The chemistry, optics and genesis of the alkali-amphiboles. *Journal of the Faculty of Science*, University of Tokyo, Section II, Pt. 1(11), 57–73.

Nesse, W.D. (Ed.) (2017). *Introduction to Mineralogy*. Oxford University Press, 3rd edition, p. 512.

Ódri, Á., Harris, C., and Le Roux, P. (2020). The role of crustal contamination in the petrogenesis of nepheline syenite to granite magmas in the Ditrău Complex, Romania: evidence from O-, Nd-, Sr- and Pb-isotopes. *Contributions to Mineralogy and Petrology*, 175: 100.

Pál-Molnár, E. (Ed.) (2000). *Hornblendites and diorites of the Ditrău Syenite Massif*. Department of Mineralogy, Geochemistry and Petrology, University of Szeged, Szeged, p. 172.

Pál-Molnár, E. (2010). Geology of Székelyland. In: Szakáll, S. and Kristály, F. (Eds.), *Mineralogy of Székelyland, Eastern Transylvania, Romania*. Csík County Nature and Conservations Society, Sfântu Gheorghe–Miercurea-Ciuc–Târgu Mureş, pp. 33–43.

Pál-Molnár, E., Batki, A., Almási, E.E., Kiss, B., Upton, B.G.J., Markl, G., Odling, N., and Harangi, Sz. (2015a). Origin of mafic and ultramafic cumulates from the Ditrău Alkaline Massif, Romania. *Lithos*, 239: 1–18.

Pál-Molnár, E., Batki, A., Ódri, Á., Kiss, B., and Almási, E.E. (2015b). Geochemical implications of the magmatic origin of granitic rocks from the Ditrău Alkaline Massif (Eastern Carpathians, Romania). *Geologia Croatica*, 68/1: 51–66.

Pál-Molnár, E., Kiri, L., Lukács, R., Dunkl, I., Batki, A., Szemerédi, M., Almási, E.E., Sogrik, E., and Harangi, S. (2021). Timing of magmatism of the Ditrău Alkaline Massif, Romania – A review based on new U-Pb and K/Ar data. *Central European Geology*, 64(1): 18–37.

Pandit, D., Panigrahi, M.K., and Moriyama, T. (2014). Constrains from magmatic and hydrothermal epidotes on crystallization of granitic magma and sulfide mineralization in Paleoproterozoic Malanjkhand Granitoid, Central India. *Chemie der Erde*, 74: 715–733.

Park, Y. and Means, W.D. (1996). Direct observation of deformation processes in crystal mushes. *Journal of Structural Geology*, 18: 847–858.

Presnall, D.C. and Bateman, P.C. (1973). Fusion relations in the system $NaAlSi_3O_8$-$CaAl_2Si_2O_8$-$KAlSi_3O_8$-SiO_2-H_2O and generation of granitic magmas in the Sierra Nevada Batholith. *Geological Society of America Bulletin*, 84: 3182–3202.

Roduit, N. (2019). JMicroVision: image analysis toolbox for measuring and quantifying components of high-definition images. Version 1.3.1. https://jmicrovision.github.io.

Săndulescu, M. (1984). *Geotectonica României*. Editura Technică, p. 336.

Săndulescu, M., Kräutner, H.G., Balintoni, I., Russo-Săndulescu, M., and Micu, M. (1981). The structure of the East Carpathians (Moldavia – Maramures area). *Guide Exc. B1, XII Congress of the Carpathian Balkan Geological Association*. Institute of Geology and Geophysics, Bucuresti, p. 92.

Streckeisen, A. (1960). On the structure and origin of the nephelinsyenite complex of Ditro (Transylvania, Roumania). *Rep. 21th IGC*, 13: 228–238.

Streckeisen, A. and Hunziker, J.C. (1974). On the origin of the nephelinsyenit Massif of Ditró (Transylvania, Romania). *Schweizerische Mineralogische und Petrographische Mitteilungen*, 54: 59–77.

Tate, M.C., Clarke, D.B., and Heaman, L.M. (1997). Progressive hybridisation between Late Devonian mafic-intermediate and felsic magmas in the Meguma Zone of Nova Scotia, Canada. *Contributions to Mineralogy and Petrology*, 126: 401–415.

Ubide, T., Galé, C., Larrea, P., Arranz, E., Lago, M., and Tierz, P. (2014). The relevance of crystal transfer to magma mixing: a case study in composite dykes from the Central Pyrenees. *Journal of Petrology*, 55(8): 1535–1559.

Vance, J.A. (1969). On synneusis. *Contributions to Mineralogy and Petrology*, 24: 7–29.

Vernon, R.H. (1984). Microgranitoid enclaves in granites–globules of hybrid magma quenched in a plutonic environment. *Nature*, 309: 438–439.

Vernon, R.H. (1990). Crystallization and hybridism in microgranitoid enclave magmas: Microstructural evidence. *Journal of Geophysical Research*, 95: 17849–17859.

Vernon, R.H. and Collins, W.J. (2011). Structural criteria for identifying granitic cumulates. *Journal of Geology*, 119: 127–142.

Vernon, R.H., Johnson, S.E. and Melis, E.A. (2004). Emplacement-related microstructures in the margin of a deformed pluton: the San José tonalite, Baja California, México. *Journal of Structural Geology*, 26: 1867–1884.

Vernon, R.H. and Paterson, S.R. (2006). Mesoscopic structures resulting from crystal accumulation and melt movement in granites. *Transactions of the Royal Society of Edinburgh: Earth Sciences*, 97(4): 369–381.

Verschure, R.H. and Maijer, C. (2005). A new Rb-Sr isotopic parameter for metasomatism, Δt, and its application in a study of pluri-fenitized gneisses around the Fen ring complex, South Norway. *Norges Geologiske Undersøkelse Bulletin*, 445: 45–71.

Vodă, A. and Balintoni, I. (1994). Corelari lithostratigrafice în cristalinul Carpaţilor Orientali. *Studia Universitates Babeş-Bolyai*, Geologia, 39: 61–66.

Vogt, J.H.L. (1921). The physical chemistry of the crystallization and magmatic differentiation of the igneous rocks. *Journal of Geology*, 29(5): 426–443.

Wall, V.J., Clemens, J.D., and Clarke, D.B. (1987). Models for granitoid evolution and source compositions. *Journal of Geology*, 95: 731–749.

White, A.J.R. and Chappell, B.W. (1977). Ultrametamorphism and granitoid genesis. *Tectonophysics*, 43: 7–22.

White, R.W., Pomroy, N.E., and Powell, R. (2005). An in situ metatexite-diatexite transition in upper amphibolite facies rocks from Broken Hill, Australia. *Journal of Metamorphic Geology*, 23: 579–602.

Whitney, D.L. and Evans, B.W. (2010). Abbreviations for names of rock-forming minerals. *American Mineralogist*, 95: 185–187.

Wiebe, R.A. (1968). Plagioclase stratigraphy; a record of magmatic conditions and events in a granite stock. *American Journal of Science*, 266: 690–703.

Wiebe, R.A. (1973). Relations between coexisting basaltic and granitic magmas in a composite dike. *American Journal of Science*, 273: 130–151.

Wiebe, R.A., Blair, K.D., Hawkins, D.P., and Sabine, C.P. (2002). Mafic injections, in situ hybridization, and crystal accumulation in the Pyramid Peak granite, California. *Bulletin of the Geological Society of America*, 114: 909–920.

Wiebe, R.A. and Collins, W.J. (1998). Depositional features and stratigraphic sections in granitic plutons: implications for the emplacement and crystallization of granitic magma. *Journal of Structural Geology*, 20(9/10): 1273–1289.

Wiebe, R.A., Smith, D., Sturm, M., King, E.M., and Seckler, M.S. (1997). Enclaves in the Cadillac Mountain Granite (Coastal Maine): samples of hybrid magma from the base of the chamber. *Journal of Petrology*, 38(3): 393–423.

Zorpi, M.J., Coulon, C., and Orsini, J.B. (1991). Hybridization between felsic and mafic magmas in calc-alkaline granitoids — a case study in northern Sardinia, Italy. *Chemical Geology*, 92: 45–86.